

**Metabolism of MRX-I, a Novel Antibacterial Oxazolidinone, in
Humans: the Oxidative Ring-opening of 2,3-Dihydropyridin-4-one
Catalyzed by Non-P450 Enzymes**

Jian Meng, Dafang Zhong, Liang Li, Zhengyu Yuan, Hong Yuan, Cen Xie, Jialan
Zhou, Chen Li, Mikhail Fedorovich Gordeev, Jinqian Liu, Xiaoyan Chen

Shanghai Institute of Materia Medica, Chinese Academy of Sciences, Shanghai,
China (J.M., D.Z., L.L., C.X., J.Z., C.L., X.C.); MicuRx Pharmaceuticals, Inc.,
Shanghai, China (Z.Y., H.Y.); and MicuRx Pharmaceuticals, Inc., Hayward, United
states (M.G., J.L.)

Running Title

Metabolism of Antibacterial Oxazolidinone MRX-I in Humans

Corresponding author: Xiaoyan Chen

Shanghai Institute of Materia Medica, Chinese Academy of Sciences, 501 Haik Road,

Shanghai, China

Phone: +86-21-50800738; Fax: +86-21-50800738;

Email: xychen@simm.ac.cn

Number of text pages: 25

Number of tables: 4

Number of figures: 11

Number of references: 19

Number of words in the Abstract: 236

Number of words in the Introduction: 348

Number of words in the Discussion: 1359

ABBREVIATIONS: FMO, flavin-containing monooxygenase; UPLC, ultraperformance liquid chromatography; Triple TOF MS, triple time-of-flight mass spectrometry; ABT, 1-aminobenzotriazole; 4-MP, 4-methylpyrazole; P450, cytochrome P450; ADH, alcohol dehydrogenase; AKR, aldo-keto reductase; SDR, short-chain dehydrogenase/reductase; ALDH, aldehyde dehydrogenase.

ABSTRACT

MRX-I is an analogue of linezolid, containing a 2,3-dihydropyridin-4-one (DHPO) ring rather than a morpholine ring. Our objectives were to characterize the major metabolic pathways of MRX-I in humans and to clarify the mechanism underlying the oxidative ring-opening of the DHPO. After an oral dose of MRX-I (600 mg), nine metabolites were identified in humans. The principal metabolic pathway proposed involved DHPO ring-opening, generating the main metabolites in the plasma and urine: the hydroxyethyl amino propionic acid metabolite MRX445-1 and the carboxymethyl amino propionic acid metabolite MRX459. An *in vitro* phenotyping study demonstrated that multiple non-P450 enzymes are involved in the formation of MRX445-1 and MRX459, including flavin-containing monooxygenase 5 (FMO5), short-chain dehydrogenase/reductase (SDR), aldehyde ketone reductase (AKR), and aldehyde dehydrogenase (ALDH). H_2^{18}O experiments revealed that two ^{18}O atoms are incorporated into MRX445-1, one in the carboxyethyl group and the other in the hydroxyl group, and three ^{18}O atoms are incorporated into MRX459, two in the carboxymethyl group and one in the hydroxyl group. Based on these results, the mechanism proposed for DHPO ring opening involves the metabolism of MRX-I via FMO5-mediated Baeyer–Villiger oxidation to an enol lactone, hydrolysis to an enol, and enol–aldehyde tautomerism to an aldehyde. The aldehyde is reduced by SDR, AKR, ALDH to MRX445-1 or oxidized by ALDH to MRX459. Our study suggests that few clinical adverse drug–drug interactions should be anticipated between MRX-I and P450 inhibitors or inducers.

Introduction

Today, antibiotic resistance is still threatening the health of many people worldwide. Therefore, it is of great urgency for the pharmaceutical industry to develop new antibiotics with better safety profiles for drug-resistant bacteria (Talbot et al., 2006). Oxazolidinone antibacterial agents bind to a distinct region of the 23S RNA adjacent to the peptidyl transferase center of the 50S ribosomal subunit and show activity against major Gram-positive pathogens (Dean, 1999). Its distinct binding site reduces the cross-resistance between oxazolidinone and other antibacterial drugs. To date, linezolid is the only oxazolidinone antibacterial agent approved by the US Food and Drug Administration for the treatment of serious Gram-positive infections, including those caused by antibiotic-resistant organisms. However, linezolid is subject to serious safety limitations. The primary safety concerns are myelosuppression and monoamine oxidase inhibition, which limit extended linezolid therapy (Vinh and Rubinstein, 2009).

MRX-I, (5*S*)-5-[(isoxazol-3-ylamino)methyl]-3-[2,3,5-trifluoro-4-(4-oxo-2,3-dihydropyridin-1-yl)phenyl]oxazolidin-2-one, is a novel oxazolidinone antibiotic currently in clinical trials in China. One of the important changes in the structure of the compound is the substitution of the morpholine heterocycle in linezolid with the more planar 2,3-dihydropyridin-4-one (DHPO) ring, which contributes to the increased antibacterial activity of MRX-I compared with that of linezolid (Gordeev and Yuan, 2014). In nonclinical studies, MRX-I demonstrated the same or better efficacy than linezolid in mouse infection models (Li et al., 2014). In preclinical toxicology studies and phase I clinical trials, MRX-I displayed less propensity to induce myelosuppression than did linezolid (Gordeev and Yuan, 2014).

Drug metabolism study is an integral and critical part of drug development.

Information, such as the major circulating metabolites and the enzymes responsible for their formation is vital for evaluating drug safety and drug–drug interactions. A preliminary metabolism study in humans demonstrated that MRX-I is mainly metabolized by an unusual metabolic pathway involving the oxidative DHPO ring-opening. Therefore, the objectives of the current study were: 1) to characterize the metabolic pathways of MRX-I in humans following an oral dose of MRX-I (600 mg); 2) to identify the enzymes involved in the DHPO ring-opening of MRX-I; and 3) to understand the DHPO ring-opening mechanism with H₂¹⁸O experiments.

Materials and Methods

Materials

MRX-I, HM5013199, HM5012569, HM5013876, HM1383, MRX-1314, and MRX-1315 were provided by MicuRx Pharmaceuticals Inc. (Shanghai, China). Methimazole, 1-aminobenzotriazole (ABT), 4-methylpyrazole (4-MP), flufenamic acid, raloxifene, allopurinol, and disulfiram were purchased from Sigma-Aldrich (St. Louis, MO, USA). Menadione was bought from Sinapharm Chemical Reagent Co., Ltd (Shanghai, China). Methotrexate was acquired from the National Institute for the Control of Pharmaceutical and Biological Products (Beijing, China). H₂¹⁸O (97 atom % ¹⁸O) was obtained from the Shanghai Research Institute of Chemical Industry (Shanghai, China).

Cryopreserved human hepatocytes, pooled human liver S9 fractions, liver cytosolic fractions, liver microsomes, and recombinant FMO Supersomes, including FMO1, FMO3, and FMO5, were purchased from BD Gentest (Woburn, CA, USA). NADPH, NADP⁺ and NAD⁺ were purchased from Sigma-Aldrich.

All solvents for the ultraperformance liquid chromatography/triple time-of-flight mass spectrometry (UPLC/Triple TOF MS) analyses were of high-performance liquid chromatography (HPLC) grade (Merck, Darmstadt, Germany). Ultrapure water was generated using a Milli-Q Gradient system (Millipore Corporation, Molsheim, France). Other reagents were of analytical grade (Shanghai Chemical Plant, Shanghai, China).

Study Protocol and Sample Collection

The human blood, urine and feces samples were collected from four healthy male subjects during the course of a Phase-I clinical trial of MRX-I conducted at the Clinical Trial Center of Shanghai Huashan Hospital. The study was conducted in

accordance with the Declaration of Helsinki, and was approved by the Ethics Committee of Huashan Hospital affiliated to Fudan University. All subjects gave their voluntary informed consent and received multiple dose of 600 mg of MRX-I (tablet) through q12h oral administration for 14 days. Blood, urine and feces samples were collected within 24 hours before receiving the first dose of MRX-I, and were collected at predetermined time points after receiving the last dose. Following the collection of blood samples, the plasma was isolated by centrifugation, and stored at -20°C until analysis. To each fecal sample was added five volumes of methanol (1 g/5 ml), followed by homogenization. The urine and feces samples were stored frozen at -20°C until analysis.

Metabolite Profiling and Identification

Preparation of Samples Plasma, urine, and feces samples were pooled and prepared for metabolite profiling. Plasma samples were segregated by sample collection time (predose, and 1.5 hours and 6 hours postdose), and equal volumes (50 μl) from each subject were pooled. The plasma proteins were precipitated by the addition of three volumes of acetonitrile, vortexed for 1 min, and centrifuged for 5 min at $11,000 \times g$. The supernatant was transferred to glass tubes and evaporated to dryness under N_2 at 40°C . The residues were reconstituted in 20% aqueous methanol (400 μl), and a 10 μl aliquot of the resulting solution was injected into the UPLC apparatus for analysis.

Urine or feces samples (predose and 0–24 hours postdose) were pooled by combining volumes proportional to the total weight excreted from each subject at each urine or feces collection interval. The pooled urine samples were centrifuged for 5 min at $11,000 \times g$ and a 10 μl aliquot of the resulting supernatant was injected into the UPLC apparatus for analysis. The pooled feces samples (500 μl) were transferred

into glass tubes for evaporation to dryness under N₂ at 40 °C. The residues were reconstituted in 20% aqueous methanol (400 μ l) and a 10 μ l aliquot of the resulting solution was injected into the UPLC apparatus for analysis.

UPLC-UV/Triple-TOF MS Analysis Chromatographic separation for the metabolite profiling and identification was conducted on an Acquity UPLC HSS T3 column (100 mm \times 2.1 mm i.d., 1.8 μ m) using an Acquity UPLC system (Waters, Milford, MA, USA). The mobile phase consisted of 0.05% formic acid in water (solvent A) and methanol (solvent B). The flow rate was maintained at 0.45 ml/min. MRX-I and its metabolites were eluted with a linear gradient of the mobile phase composition, as follows: 5% solvent B for 5 min, a linear gradient to 40% solvent B at 17 min, held at 40% solvent B until 20 min, a linear gradient to 100% solvent B at 22 min, and reequilibration of the column to 5% solvent B for 4 min. The eluted fractions were monitored by UV detection at 254 nm.

MS detection was achieved using a Triple TOF 5600+ MS/MS system (AB Sciex, Concord, Ontario, Canada) in the positive ESI mode. The mass range was set at m/z 100–1000. The following parameter settings were used: ion spray voltage, 5500 V; declustering potential, 60 V; ion source heater, 550 °C; curtain gas, 40 psi; ion source gas 1, 55 psi; and ion source gas 2, 50 psi. For the TOF MS scans, the collision energy (CE) was 10 eV; for product ion scans, CE was 35 eV with a spread of 15 eV in the MS/MS experiment. Information-dependent acquisition (IDA) was used to trigger the acquisition of MS/MS spectra for ions matching the IDA criteria. A real-time multiple mass defect filter was used for the IDA criteria.

Metabolite Isolation and NMR Spectral Characterization

Metabolites MRX445-1 and MRX445-2 were isolated from human urine. Briefly, a pooled urine sample (approximately 800 ml) from one subject was concentrated to

approximately 100 under vacuum, and then fractionated using YMC*GEL ODS-A-HG column chromatography (0 – 100% anhydrous methanol), yielding seven fractions (A–G). Fraction E, eluted with water:methanol (3:7, v/v), was further purified on a Shimadzu LC-6AD semipreparative HPLC apparatus using a YMC-Pack ODS-A column (10 × 250 mm, 5 mm i.d.; YMC Company Ltd., Kyoto, Japan) detected at 254 nm with an SPD-20A UV detector. The mobile phase was a mixture of 5 mM ammonium acetate and acetonitrile (87:13, v/v), with a flow rate of 2.0 ml/min. Fraction E produced MRX445-1 (22 mg) and MRX445-2 (2.1 mg). Using a similar method to those used to isolate MRX445-1 and MRX445-2, metabolite MRX413 (5 mg) was isolated from the feces homogenate.

The structures of MRX445-1, MRX445-2, and MRX413 were characterized with ¹H and ¹³C NMR. These compounds were dissolved into dimethylsulfoxide-d₆ and the NMR measurements were made on a Bruker AVANCE III-400 (Newark, DE, USA) using tetramethylsilane as the internal standard. The NMR data for MRX-I were acquired under the same conditions.

Metabolism of MRX-I *In Vitro*

Incubation of MRX-I in Human Liver Microsomes, Cytosol, or S9 Fractions

The MRX-I in methanol stock solution was added to 200 μ l of potassium phosphate buffer (0.1 M, pH 7.4), at a final concentration of 10 μ M (final methanol 0.5%). A stock solution of NADPH was also added to a final concentration of 2.0 mM. The mixture was preincubated at 37 °C for 3 min. The reactions were initiated by the addition of ice-cold human liver microsomes at a final protein concentration of 0.5 mg/ml, human liver cytosol at a final protein concentration of 2.0 mg/ml, or human liver S9 fractions at a final protein concentration of 2.5 mg/ml. The mixtures were incubated at 37 °C for 120 min. Each reaction was quenched by the addition of an

equal volume of acetonitrile with subsequent centrifugation ($11,000 \times g$, 5 min, 4 °C). The supernatant was dried under a stream of nitrogen at 40 °C, reconstituted in 20% aqueous methanol (200 μ l) and then analyzed by UPLC/Triple TOF MS, as described above for metabolite profiling.

Enzymes Phenotyping Involved in DHPO Ring-opening To determine the enzymes responsible for the formation of metabolites related to MRX-I DHPO ring-opening, various specific phenotypic inhibitors were added to the S9 fraction incubation system: ABT (1000 μ M final concentration, P450 inhibitor), methimazole (100 μ M final concentration, P450 and FMO inhibitor, except FMO5), menadione (1 – 100 μ M final concentration, aldehyde oxidase [AO] and short-chain dehydrogenase reductase [SDR] inhibitor) (Morrison et al., 2012; Rosemond and Walsh, 2004), raloxifene (0.001 – 100 μ M final concentration, AO inhibitor), methotrexate (50 μ M final concentration, xanthine oxidase [XO] inhibitor), allopurinol (100 μ M final concentration, XO inhibitor) (Morrison et al., 2012), 4-MP (100 μ M final concentration, alcohol dehydrogenase [ADH] inhibitor), flufenamic acid (100 μ M final concentration, aldo-keto reductase [AKR] inhibitor) (Rosemond and Walsh, 2004) and disulfiram (50 μ M final concentration, aldehyde dehydrogenase [ALDH] inhibitor) (Stagos et al., 2010). After these inhibitors were incubated with human liver S9 fractions in the presence of NADPH for 15 min, the MRX-I in methanol stock solution was added to the incubation system. NAD^+ was also supplemented when 4-MP was used as an ADH inhibitor and NADP^+ for disulfiram as an ALDH inhibitor. To test the involvement of the thermally unstable FMOs in the oxidation reaction, human liver S9 fractions were preincubated at 50 °C for 5 min in the absence of NADPH and then added to the incubation system. The samples were incubated at 37 °C for 120 min and then processed and analyzed by UPLC/Triple TOF MS as

described above.

Incubation of MRX-I in Liver Cytosol-fortified Recombinant FMOs The MRX-I in methanol stock solution was added at a final concentration of 10 μ M (final methanol 0.5%) to a final volume of 200 μ L of potassium phosphate buffer (0.1 M, pH 7.4). A stock solution of NADPH and a stock solution of human liver cytosol were also added at final concentrations of 2.0 mM and 1 mg/ml, respectively. The mixtures were preincubated at 37 °C for 3 min, and the reactions were initiated by the addition of ice-cold recombinant FMO1, FMO3, or FMO5 Supersomes at a final protein concentration of 0.5 mg/ml. The mixtures were incubated at 37 °C for 120 min, quenched by the addition of an equal volume of acetonitrile, and then centrifuged (11,000 \times g, 5 min, 4 °C). The resulting supernatant was dried under a stream of nitrogen at 40°C, reconstituted in 20% aqueous methanol (200 μ l), and then analyzed by UPLC/Triple TOF MS as described above.

H₂¹⁸O Incorporation into the DHPO ring-opened Metabolites To probe the presence of the aldehyde intermediate, the incorporation of oxygen from the medium into the metabolites was assessed by incubation of MRX-I (10 μ M) with liver cytosol-fortified FMO5 supplemented with NADPH (2.0 mM) containing H₂¹⁸O (90% v/v). The reactions were incubated at 37 °C for 120 min and quenched by the addition of an equal volume of acetonitrile. For comparison, the DHPO ring-hydrogenated MRX-I, MRX-1314, was also subjected to the same *in vitro* experiment as MRX-I. The samples were processed and analyzed by UPLC/Triple TOF MS, as described above, to assess the incorporation of H₂¹⁸O into the metabolites, including MRX445-1, MRX445-2, and MRX459.

Incubation of MRX-I and MRX-1314 with Human Hepatocytes. The metabolism of MRX-I and MRX-1314 was evaluated in human hepatocytes. The

DMD # 61747

reactions were incubated in Williams' E medium at a hepatocyte density of 1×10^6 cells/ml. The final MRX-I or MRX-1314 concentration in the cell suspension was 10 μ M in a volume of 200 μ l. The reactions were incubated at 37 °C for 120 min, quenched by the addition of an equal volume of acetonitrile, and then centrifuged ($11,000 \times g$, 5 min, 4 °C). The resulting supernatant was dried under a stream of nitrogen at 40 °C, reconstituted in 20% aqueous methanol (200 μ l), and then analyzed by UPLC/Triple TOF MS as described above.

Results

UPLC/Triple TOF MS Analysis of MRX-I

The chromatographic and MS fragmentation behaviors of the parent drug, MRX-I, was first investigated to identify MRX-I metabolites. MRX-I was eluted at 17.2 min under the chromatographic conditions employed. In ESI (+) mode, MRX-I gave a protonated molecular ion at m/z 409.1111. The main characteristic product ions of m/z 409.1111 were observed at m/z 365.1219, 281.0899, 255.0749, 251.0790, 243.0736, and 123.0549. The fragment ion at m/z 365.1219 was proposed to be the result of the loss of CO₂ from MRX-I, the fragment ions at m/z 281.0899, 255.0749, 251.0790, and 243.0736 formed by the cleavage of the oxazolidinone ring, whereas the fragment ion at m/z 123.0549 from the part of the isoxazole amine of MRX-I, based on the high-resolution mass spectral information (Table 1, Supplemental Figure 1).

MRX-I Metabolite Profiling and Identification

MRX-I and its metabolites in humans were determined by UPLC-UV/Triple TOF MS. In addition to MRX-I, seven metabolites were identified in the pooled human plasma (Fig. 1) and urine (Fig. 2), whereas nine metabolites were detected in human feces (Fig. 3). The metabolite profile of human plasma at 6 hours postdose was not shown, for it was similar to that at 1.5 hours. Although metabolic modifications of the parent drug usually result in different ionization efficiency and UV absorption coefficient, the MS response and UV absorbance roughly reflect the relative quantity of the metabolites. As shown in Fig. 1, the most abundant circulating drug-related component was the parent drug. The predominant metabolites in the plasma were MRX445-1 and MRX459, eluted at 16.2 min and 16.1 min, respectively. The plasma concentrations of MRX-I, MRX445-1 and MRX459 were determined by a LC-MS/MS method and the plasma exposures of MRX445-1 and MRX459 were 26.4%

and 24.0% of the parent drug exposure (data not shown). Furthermore, MRX445-1 and MRX459 were also the main drug-related materials detected in the urine (Fig. 2). A large amount of unchanged parent drug was detected in feces, and the major metabolite detected was MRX413, eluted at 9.3 min (Fig. 3).

Table 1 lists detailed information about these metabolites, including the proposed structures, protonated molecular ions, retention times, and the characteristic fragment ions. The metabolites were named in accordance with their protonated molecular weights, and metabolites with the same molecular weight were named in the sequential order of their retention times. The metabolites were identified as follows.

Parent Drug M0. A chromatographic peak was detected at 17.2 min in human plasma, urine, and feces. It gave a protonated molecular ion at m/z 409.1111, indicating that its elemental composition was $C_{18}H_{15}N_4O_4F_3$. The retention time and mass spectral fragmentation patterns were identical to the parent drug, MRX-I, indicating that this component was unmetabolized MRX-I, designated M0.

MRX343. Metabolite MRX343, found in plasma, urine and feces, was eluted at 14.1 min, with a protonated molecular mass of 343.0895. The elemental composition of MRX343 was $C_{15}H_{13}N_2O_4F_3$. The fragment ions at 255.0737 and 251.0788 were the same as those of MRX-I. The fragment ion at m/z 123.0549 was not detected, indicating that the isoxazole amine was lost from the parent drug. The fragment ion at m/z 325.0795 was proposed to be the result of the neutral loss of H_2O from MRX343. The chromatographic retention time and mass spectral fragmentation patterns of MRX343 were identical to those of HM5013199, so MRX343 was accordingly confirmed as the deaminated metabolite of MRX-I.

MRX357. Metabolite MRX357, found in plasma, urine, and feces, was eluted at 15.1 min and had a protonated molecular mass of 357.0693, with an elemental

composition of $C_{15}H_{11}N_2O_5F_3$. The fragment ion at 251.0787 was the same as that of MRX-I. The fragment ion at m/z 123.0549 was not detected, indicating that the isoxazole amine was lost from the parent drug. The fragment ion at m/z 339.0587 was proposed to be the result of the neutral loss of H_2O from MRX357. The chromatographic retention time and mass spectral fragmentation pattern of MRX357 were identical to those of HM5012596, the authentic standard. MRX357 was therefore confirmed as the carboxylic acid metabolite of MRX-I, formed by oxidative deamination.

MRX407. Metabolite MRX407 was found in plasma, urine, and feces, and was eluted at 14.2 min. It had a protonated molecular mass of 407.0962 with an elemental composition of $C_{18}H_{13}N_4O_4F_3$, indicating that MRX407 was the dehydrogenated metabolite of MRX-I. The fragment ion at m/z 123.0553 was the same as that of MRX-I. The fragment ions at 363.1061, 279.0737, 253.0585, and 241.0579 were 2 Da smaller than those of the parent drug, indicating that dehydrogenation occurred on the DHPO ring. The chromatographic retention time and mass spectral fragmentation pattern of MRX407 were identical to those of HM5013876. MRX407 was accordingly confirmed as DHPO ring-dehydrogenated MRX-I.

MRX413. Metabolite MRX413 was only found in feces and was eluted at 9.3 min. It had a protonated molecular mass of 413.1428, with an elemental composition of $C_{18}H_{19}N_4O_4F_3$. The fragment ion at m/z 255.0733 was the same as that of MRX-I, indicating that the DHPO ring and trifluorobenzene moieties were not modified. The fragment ion at m/z 369.1528 was a result of the neutral loss of CO_2 from MRX413 and the fragment ion at m/z 339.1426 was proposed to result from the further loss of CH_2O from the fragment ion at m/z 369.1528. The fragment ion at m/z 123.0549 was not present, indicating that the isoxazole ring was modified. The structure of MRX413

was further characterized by NMR after the metabolite was isolated from human feces. The ^1H and ^{13}C NMR data are listed in Table 2 and 3, respectively. Comparison of the chemical shifts of MRX413 with those of MRX-I, it was shown that the DHPO ring and trifluorobenzene moieties were unchanged. However, the sp^2 -hybridized methine signals of isoxazole disappeared and new signals from a methylene group attached to an oxygen atom (i.e., δ_{C} 58.2, δ_{H} 3.88, CH_2 -18) and a methylene group (i.e., δ_{C} 35.9, δ_{H} 2.72, CH_2 -17) appeared. The structure of MRX413 was further confirmed as the reduced isoxazole ring-opened metabolite with ^1H - ^1H COSY, HMBC, and HSQC (Table 1, Supplemental Figure 5).

MRX445-1. Metabolite MRX445-1 was the most prominent metabolite in plasma and urine, and was also found in feces. MRX445-1 was eluted at 16.2 min and had a protonated molecular mass of 445.1322 with an elemental composition of $\text{C}_{18}\text{H}_{19}\text{N}_4\text{O}_6\text{F}_3$, indicating the dihydration ($2\text{H}_2\text{O}$) of MRX-I. The mass spectrum of m/z 445.1322 gave major fragment ions at m/z 427.1224, 385.1109, 341.0863, and 123.0555. The fragment ion at m/z 427.1224 was the result of the loss of H_2O from MRX445-1. The fragment ion at m/z 123.0555 was the same as that of the parent drug, indicating that the isoxazole ring was not modified. However, the major fragment ions at m/z 365.1219, 281.0899, 255.0749, and 243.0736 of MRX-I were not found in MRX445-1, indicating that the DHPO ring might be modified. The structure of MRX445-1 was further characterized by NMR after the metabolite was isolated from human urine. The ^1H and ^{13}C NMR data are listed in Table 2 and 3, respectively. Comparison of the chemical shifts of MRX445-1 with those of MRX-I showed that the trifluorobenzene, oxazolidinone, and isoxazole amine moieties were unchanged. However, the characteristic NMR signals of the MRX-I DHPO ring had disappeared in MRX445-1. Signals appeared indicating a new hydroxylethyl group (δ_{C} 59.8, δ_{H}

3.14, CH₂-1; δ_C 55.5, δ_H 3.20-3.50, CH₂-2) and carboxyethyl group (δ_C 49.4, δ_H 3.20-3.50, CH₂-3; δ_C 33.7, δ_H 2.33, CH₂-4; δ_C 173.4, C-5). Therefore, MRX445-1 was identified with ¹H-¹H COSY, HMBC, and HSQC NMR (Supplemental Figure 3) as the hydroxyethyl amino propionic acid metabolite formed by the oxidative opening of the DHPO ring (Table 1). This structure was confirmed with its synthesized standard. The fragment pathways of MRX445-1 are shown in Table 1. The fragment ions at m/z 385.1109 and 341.0863 were proposed to be the result of the neutral loss of C₂H₄O₂ and C₂H₄O₂C₂H₄O from MRX445-1, respectively.

MRX401. Metabolite MRX401 was found in plasma, urine and feces, and was eluted at 17.1 min. It had a protonated molecular mass of 401.1070, with an elemental composition of C₁₆H₁₅N₄O₅F₃. The fragment ions at m/z 341.0860 and 123.0555 were the same as those of MRX445-1, indicating that the trifluorobenzene, oxazolidinone, and isoxazole amine moieties were not modified. However, the fragment ion at m/z 385.1109 was not detected, indicating the loss of the hydroxyethyl group from MRX445-1. MRX401 was accordingly identified as *N*-dehydroxyethyl MRX445-1.

MRX459. Metabolite MRX459 was eluted at 16.1 min and was a major metabolite in plasma and urine, also found in feces. It had a protonated molecular mass of 459.1114, with an elemental composition of C₁₈H₁₅N₄O₇F₃, indicating the introduction of an oxygen atom accompanied by dehydrogenation relative to MRX445-1. The fragment ions at m/z 341.0860, 187.0473, and 123.0555 were the same as those of MRX445-1, suggesting that the trifluorobenzene, oxazolidinone, and isoxazole amine moieties were not modified. The fragment ion at m/z 385.1109 was not observed but a fragment ion at m/z 399.0902 (+14 Da) appeared. A fragment ion derived from decarboxylation was also observed at m/z 413.1059. The chromatographic retention time and mass spectral fragmentation pattern of MRX459

were identical to those of HM1383. Therefore, MRX459 was identified as oxidized MRX445-1, where the hydroxyethyl group was converted to a carboxylic acid (Table 1).

MRX445-2. Metabolite MRX445-2, found in plasma, urine, and feces, was eluted at 16.7 min and had a protonated molecular mass of 445.1316, the same as that of MRX445-1. Although MRX445-2 had the same elemental composition as MRX445-1, it produced different fragment ions. The structure of MRX445-2 was characterized by NMR after the metabolite was isolated from human urine. The ^1H and ^{13}C NMR data are listed in Table 2 and 3. Comparison of the chemical shifts of MRX445-2 with those of MRX-I and MRX445-1 showed that the trifluorobenzene, oxazolidinone, and isoxazole amine moieties were unchanged. Like MRX445-1, the characteristic NMR signals of the DHPO ring of MRX-I had disappeared in MRX445-2. New signals from a carboxyl group (δ_{C} 173.5, C-2), methylene group (δ_{C} 37.8, δ_{H} 2.34, and 2.27, C-1), and a methine attached to an oxygen atom (δ_{C} 65.7, δ_{H} 3.92, CH-5) had appeared. The ^1H NMR spectrum of MRX445-2 revealed the presence of two active NH protons (δ_{H} 6.59 and 5.61), indicating the opening of the DHPO ring at the C–N bond. The introduction of NH shifted the C-3 and C-11 signals upfield from δ_{C} 49.6 to 43.1 and from δ_{C} 121.8 to 113.5, respectively. The reduction of the carbonyl group on C-5 shifted the C-4 signals downfield from δ_{C} 36.5 to 42.3 (Supplemental Figure 4). MRX445-2 was accordingly identified as the 5-amino-3-hydroxypentanoic acid metabolite of MRX-I formed by the opening of the DHPO ring (Table 1).

MRX427. Metabolite MRX427, found only in feces, was eluted at 13.6 min. It had a protonated molecular mass of 427.1227 with an elemental composition of $\text{C}_{18}\text{H}_{17}\text{N}_4\text{O}_5\text{F}_3$. The mass spectrum of m/z 427.1 showed major fragment ions at m/z 409.1119, 368.0851, 281.0889, 243.0727, and 123.0544. In the product ion spectrum

of m/z 427.1, the fragment ion at m/z 409.1119 was a result of the neutral loss of H_2O (-18.0108 Da) from MRX427, indicating that MRX427 might contain an alcoholic hydroxyl group. The fragment ions at m/z 281.0889, 243.0727 and 123.0544 were the same as those of MRX-I. The exact structure of MRX427 needs to be further characterized.

Formation of MRX445-1 and MRX459 Cocatalyzed by Enzymes in Human Liver Microsomes and Cytosolic Fractions. After MRX-I was incubated with human liver microsomes in the presence of NADPH for 120 min, traces of oxidatively deaminated metabolites of MRX-I, such as MRX343, were detected by UPLC/Triple TOF MS. The formation of DHPO ring-opened metabolites, including MRX445-1, MRX445-2, and MRX459, was not observed in the human liver microsomes (Fig. 4A). After MRX-I was incubated with human liver cytosolic fractions in the presence of NADPH for 120 min, only MRX445-2 was produced, without the major metabolites in humans, MRX445-1 and MRX459 (Fig. 4B). However, all the DHPO ring-opened metabolites detected in humans, including MRX445-1, MRX445-2, and MRX459, were observed after MRX-I was incubated with human liver S9 fractions for 120 min (Fig. 4C). These results indicate that liver microsomal or cytosolic enzymes alone do not allow the biotransformation of MRX-I to MRX445-1 and MRX459, whereas S9 fractions provided the necessary enzyme systems to complete the metabolic pathways. The enzymes in liver microsome and cytosolic fractions cocatalyzed the opening of the DHPO ring of MRX-I.

Chemical Inhibition of the Formation of MRX445-1, MRX445-2, and MRX459 in S9 Fractions. MRX-I was incubated with the NADPH-supplemented human liver S9 fractions in the presence of various specific chemical inhibitors to investigate the enzymes involved in the formation of MRX445-1, MRX445-2, and MRX459. As

shown in Table 4, ABT and methimazole did not significantly inhibit the formation of MRX445-1, MRX445-2, and MRX459, revealing that the oxidative opening of the DHPO ring was not catalyzed by P450, FMO1, FMO2, FMO3, and FMO4. However, the formation of MRX445-1 and MRX459 was reduced to 7.22% and 0%, respectively, after brief preincubation of liver S9 fractions at 50 °C in the absence of the cofactor. This indicates FMOs, other than FMO1, FMO2, FMO3, and FMO4, are involved in the formation of MRX445-1 and MRX459. Menadione, flufenamic acid and disulfiram reduced the formation of MRX445-1 to 44.6%, 69.4 and 80.0%, respectively in liver S9 fractions, whereas 4-MP had no effect on the formation of MRX445-1. This indicates that the reduction of the carbonyl group could be a step in the formation of MRX445-1 from MRX-I, catalyzed by multiple enzymes including SDR, AKR and ALDH. Furthermore, disulfiram also decreased the formation of MRX459 to 10.7%, suggesting that the oxidation of the aldehyde intermediate could be a step of the formation of MRX459, catalyzed by ALDH. The XO inhibitors, methotrexate and allopurinol, did not affect the formation of MRX445-2 from MRX-I. However, the formation of MRX445-2 was concentration-dependently inhibited by the AO inhibitors, Menadione ($IC_{50} = 8.0 \mu M$) and raloxifene ($IC_{50} = 0.66 \mu M$), respectively, as shown in Supplemental Figure S6. These indicated that AO is involved in the formation of MRX445-2.

Formation of MRX445-1, MRX445-2, and MRX459 by Incubation of MRX-I with Liver Cytosol-ortified FMO5. After MRX-I was incubated with liver cytosol-fortified FMO1, FMO3, or FMO5 in the presence of NADPH for 120 min, MRX445-2 was produced from MRX-I (Fig. 5). This is consistent with the results of incubating MRX-I with human liver cytosolic fractions and the chemical inhibition of MRX445-2 formation, which demonstrated that the formation of MRX445-2 was

catalyzed by AO and XO in the liver cytosolic fractions, not by oxidative enzymes in the liver microsomes. The formation of MRX445-1 and MRX459 was not observed during the incubation of MRX-I with liver cytosol-fortified FMO1 or FMO3, but with liver cytosol-fortified FMO5. This confirms that FMO5 is involved in the formation of MRX445-1 and MRX459, as shown in the inhibition experiments for MRX445-1 and MRX459 formation in the human liver S9 fractions.

Water is the Source of Oxygen Atoms in DHPO Ring-opened Metabolites. To explore the mechanism of oxidative DHPO ring-opening, MRX-I and DHPO ring-hydrogenated MRX-I (MRX-1314) were incubated with liver cytosol-fortified FMO5 in the presence of H_2^{18}O . UPLC/Triple TOF MS analysis clearly showed that MRX445-1 derived from MRX-I had a protonated molecular weight of 449.1303 (Fig. 6B), suggesting that two atoms of ^{18}O from H_2^{18}O were incorporated into MRX445-1 by comparing the protonated molecular weight of MRX445-1 (445.1322) in the absence of H_2^{18}O (Fig. 6A). MS/MS analysis of the protonated molecular ion at m/z 449.1 showed major fragment ions at m/z 387.1065 and 341.0760. The fragment ion at m/z 387.1065 resulted from the loss of $\text{CH}_3\text{CO}^{18}\text{OH}$ and the fragment ion at m/z 341.0760 arose from the further loss of $\text{CHCH}_2^{18}\text{OH}$. This reveals that one ^{18}O atom was incorporated into the hydroxylethyl group and the other ^{18}O atom was incorporated into the carboxylethyl group of MRX445-1 obtained from MRX-I (Fig. 6B). The UPLC/Triple TOF MS analysis also showed that MRX445-1 obtained from MRX-1314 had a protonated molecular weight of 449.1307 (Fig. 6C), suggesting that two ^{18}O atoms from H_2^{18}O were incorporated into MRX445-1. MS/MS analysis of the protonated molecular ion at m/z 449.1 showed the major fragment ions at m/z 385.1017 and 341.0762. The fragment ion at m/z 385.1017 was a result of the loss of $\text{CH}_3\text{C}^{18}\text{O}^{18}\text{OH}$. This indicates that two ^{18}O atoms from H_2^{18}O were incorporated into

the carboxylethyl group of MRX445-1 obtained from MRX-1314 (Fig. 6C). These results demonstrate that the ring opening of MRX-I and MRX-1314 occurred via different routes.

The UPLC/Triple TOF MS analysis showed that MRX445-2 from MRX-I had a protonated molecular weight of 449.1296 (Fig. 6E). Comparison of the protonated molecular weight of MRX445-2 in the absence of H_2^{18}O (445.1316) suggests that two ^{18}O atoms from H_2^{18}O were incorporated into MRX445-2 (Fig. 6D). MS/MS analysis of the protonated molecular ion at m/z 449.1 showed major fragment ions at m/z 429.1146, 411.1043, and 341.0765. The fragment ion at m/z 429.1146 was the result of the loss of H_2^{18}O ; the fragment ion at m/z 411.1048 was the result of the further loss of H_2O ; and the fragment ion at m/z 341.0767 was the result of the loss of $\text{CH}_3\text{CH}_2\text{CHOHCH}_2\text{C}^{18}\text{O}^{18}\text{OH}$. This indicates that two ^{18}O atoms from water were incorporated into the carboxyl group of MRX445-2 (Fig. 6E).

The UPLC/Triple TOF MS analysis showed that MRX459 from MRX-I had a protonated molecular weight of 465.1118 (Fig. 6G). Comparison of the protonated molecular weight of MRX459 in the absence of H_2^{18}O (459.1114) (Fig. 6F) suggests that three ^{18}O atoms from H_2^{18}O were incorporated into MRX459. MS/MS analysis of the protonated molecular ion at m/z 465.1 showed major fragment ions at m/z 415.0993, 403.0888, and 341.0768. The fragment ion at m/z 415.0993 resulted from the loss of $\text{CH}^{18}\text{O}_2\text{H}$; the fragment ion at m/z 403.0888 resulted from the loss of $\text{CH}_3\text{C}^{18}\text{OOH}$; and the fragment ion at m/z 341.0758 was formed by the neutral loss of $\text{CH}_2\text{CO}^{18}\text{OHCH}_2\text{C}^{18}\text{O}^{18}\text{OH}$. This shows that one ^{18}O atom was incorporated into the carboxylethyl group and that the other two atoms were incorporated into the carboxylmethyl group of MRX459 (Fig. 6G). Incubating MRX-1314 with human liver cytosol-fortified FMO5 did not produce MRX459 or MRX445-2.

Marked Metabolic Differences between MRX-I and MRX-1314 in Human Hepatocytes. The formation of MRX445-1 in the H₂¹⁸O experiments showed that the opening of the DHPO ring in MRX-I and MRX-1314 occurs via different routes. To clarify the possible mechanisms further, MRX-I and MRX-1314 were incubated with human hepatocytes, which contain all the liver enzymes in the liver and provide a more representative system than other *in vitro* liver models. After the incubation of MRX-I with human hepatocytes, all the DHPO ring-opened metabolites detected in humans were observed, including MRX445-1, MRX445-2, MRX459, and MRX401 (Fig. 7A). Furthermore, MRX445-1 was identified as the principle metabolite of MRX-I, as was observed *in vivo*. MRX445-1 was also present in the MRX-1314 incubation system at a similar level to that in the MRX-I incubation system (Fig. 7B). However, most of the MRX-1314 in the human hepatocyte incubation system was reduced to MRX-1315, which was not observed in the MRX-I incubation system. MRX459 was also not detected in the MRX-1314 incubation system. This demonstrates further significant metabolic differences between MRX-I and MRX-1314.

Discussion

The metabolism of MRX-I, a novel antibiotic oxazolidinone for treatment of Gram-positive infections, was studied by UPLC-UV/Triple TOF MS analysis after an oral dose of 600 mg of MRX-I to healthy male volunteers during phase I clinical trials. Nine metabolites were detected and six were confirmed with synthesized or isolated reference standards. The proposed metabolic processes are shown in Scheme 1. The oxidative ring-opening of the DHPO is the main metabolic pathway of MRX-I in humans, via which the major metabolites MRX445-1, MRX445-2, and MRX459 were formed. To identify the enzymes involved in the DHPO ring-opening, MRX-I was incubated with various *in vitro* human liver models, including liver microsomes, cytosol, S9 fractions, and primary hepatocytes. By coincubating MRX-I with various specific chemical inhibitors in the human liver S9 fractions, the enzymes involved were identified as FMOs, AKR, SDR, ALDH, and AO. The involvement of FMO5 in the formation of MRX445-1 and MRX459 was further confirmed by incubating MRX-I with liver cytosol-fortified FMOs, including FMO1, FMO3, and FMO5.

As a group of important drug-metabolizing enzymes, FMOs catalyze oxidative reactions that are complementary to P450-mediated biotransformations (Benedetti et al., 2006). Among the isoforms identified, FMO3 and FMO5 are recognized as the major isoforms in adult human liver (Zhang and Cashman, 2006; Overby et al., 1997). Typical FMO-catalyzed reactions have long been recognized, including the monooxygenation of heteroatoms such as nitrogen, sulfur, and phosphorus (Benedetti et al., 2006; Cashman 2008). However, recent studies have shown that FMO5 specifically catalyzes the Baeyer–Villiger oxidation of piperidine-4-one (Lai et al., 2011) and cyclic α,β -unsaturated ketone moieties (Verhoeven et al., 1998). Verhoeven et al. also proposed that the ring-opening mechanism of cyclic α,β -unsaturated

ketones involved the reduction of the double bond of the unsaturated ketone followed by Baeyer–Villiger oxidation catalyzed by FMOs. By analogy with previous reports, we proposed that the mechanism for DHPO ring-opening of MRX-I was as follows. MRX-I is first reduced to MRX-1314 by liver cytosolic reductases, followed by ring-expanding oxidation to a lactone via the Baeyer–Villiger reaction in liver microsomes. The lactone was then hydrolyzed to produce MRX445-1, which can be further oxidized to MRX459 (Scheme 2).

To test the proposed mechanism, the DHPO ring-hydrogenated metabolic intermediate, MRX-1314, was synthesized and incubated with human hepatocytes *in vitro* and compared with MRX-I. Although similar levels of MRX445-1 were produced independently when MRX-I and MRX-1314 were used as substrates, marked differences between MRX-I and MRX-1314 metabolism were observed. In the hepatocyte system, most of the MRX-1314 was converted to its carbonyl-reduced metabolite, MRX-1315, which indicates that the reduction of ketone is the principal metabolic pathway of MRX-1314. However, MRX-1315 was not detected in the MRX-I incubation systems. This suggests that MRX-1314 is not the metabolic intermediate in the formation of MRX445-1 from MRX-I. Furthermore, during its incubation with human hepatocytes, some MRX-I was transformed into MRX459, which could be formed by the further oxidation of the hydroxylethyl group on MRX445-1, because the oxidation of primary alcohols to carboxylic acids is one of the most common metabolic pathways of drugs in humans. However, no MRX459 was detected in the MRX-1314 incubation system, although the level of MRX445-1 produced in the MRX-1314 system was similar to that produced in the MRX-I system. This can be explained by the presence of an aldehyde intermediate in the MRX-I incubation system, from which MRX445-1 is formed by reduction and MRX459 is

formed by oxidation. This is plausible because menadione (SDR inhibitor), flufenamic acid (AKR inhibitor), and disulfiram (ALDH) inhibited the formation of MRX445-1 and disulfiram (ALDH) inhibited the formation of MRX 459 from MRX-I (Table 4). Therefore, we propose a novel metabolic mechanism (Scheme 3) for the formation of MRX445-1 and MRX459. MRX-I is metabolized to an enol lactone via Baeyer–Villiger oxidation, hydrolyzed to an enol, and transformed to an aldehyde by enol–aldehyde tautomerism, after which the aldehyde intermediate is reduced to MRX445-1 or oxidized to MRX459.

In the Baeyer–Villiger oxidation of α,β -unsaturated ketones, vinyl migration is generally favored over alkyl migration to produce ring-expanded enol lactones (Shono et al., 1974; Krafft and Katzenellenbogen, 1981), which supports the mechanism proposed in Scheme 3. Although the regiochemical selectivity of Baeyer–Villiger oxidation is recognized in chemistry, this is the first observation of the metabolism of xenobiotics to an aldehyde intermediate by direct Baeyer–Villiger oxidation of an α,β -unsaturated ketone and hydrolysis of the enol lactone. To confirm the existence of the aldehyde intermediate, MRX-I or MRX-1314 was incubated in liver cytosol-fortified recombinant FMO5 in the presence of H_2^{18}O . The isotope experiment revealed that the MRX445-1 produced from MRX-I had incorporated two ^{18}O atoms derived from water, one in the carboxyethyl group and the other in the hydroxyethyl group. Because Baeyer–Villiger oxidation is catalyzed specifically by FMO5, an oxygenase, the hydroxyethyl oxygen atom of MRX445-1 should be derived from O_2 rather than from H_2O . Therefore, the ^{18}O atom of the hydroxyethyl group of MRX445-1 indicates the existence of an aldehyde intermediate, which incorporated an ^{18}O atom from H_2^{18}O during nonenzymatic equilibrium with its geminal diol (Scheme 3). It is clear that the hydroxyl ^{18}O atom of the carboxylic acid

was derived from H_2^{18}O during the hydrolysis of the enol lactone. The isotope experiments also demonstrated that the MRX445-1 produced from MRX-1314 incorporated two ^{18}O atoms derived from H_2^{18}O . However, both atoms were incorporated in the carboxyethyl group, which differed from the results for the MRX445-1 produced from MRX-I. The carbonyl oxygen of the carboxyethyl group incorporated an ^{18}O atom because the ketone ^{16}O atom was exchanged with the H_2^{18}O ^{18}O atom during ketone–geminal diol equilibrium (Scheme 4). Furthermore, MRX-1315 with an ^{18}O -labeled hydroxyl group was the main metabolite of MRX-1314 in the presence of H_2^{18}O , which also indicates that ketone–geminal diol equilibrium of MRX-1314 occurred (data not shown). MRX445-1 produced from MRX-1314 incorporated an ^{18}O atom in the hydroxyl group of the carboxyethyl group during lactone hydrolysis, which was identical to the results for MRX445-1 produced from MRX-I.

MRX459 incorporated three ^{18}O atoms from H_2^{18}O was produced when MRX-I was incubated with liver cytosol fortified-FMO5 in the presence of H_2^{18}O . Two ^{18}O atoms were incorporated in the carboxyl hydroxyl groups of MRX459. The other ^{18}O atom was on the carboxymethyl carbonyl group, which could be incorporated during the oxidation of the aldehyde intermediate to the carboxylic acid (Scheme 3). This indicates that not oxygenases but oxidases, such as AO, OX and ALDH (Uetrecht and Trager, 2007), are involved in the formation of M459, because the incorporated oxygen atom into substrates by these enzymes are from H_2O rather than from O_2 . The involvement of ALDH in the formation of MRX459 was confirmed that disulfiram reduced the formation of MRX459 from MRX-I to 10.7%. The reaction phenotyping experiments showed that menadione and raloxifene reduced the formation of MRX445-2 with the IC_{50} values of 8.0 μM and 0.66 μM , respectively. This suggests

that AO catalyzed the formation of MRX445-2. The involvement of AO in the formation of MRX445-2 was also supported by the H₂¹⁸O experiments. After MRX-I was incubated with human liver cytosol fortified-FMO5 in the presence of H₂¹⁸O, two ¹⁸O atoms were incorporated into MRX445-2, one in the carbonyl group of carboxylic acid, which indicates that the carbon was oxidized by AO (Scheme 3).

Finally, we have characterized the metabolism of MRX-I in humans. The major metabolic pathway of MRX-I involves the oxidative opening of the DHPO ring. The mechanism underlying the directed opening of the DHPO ring proposed is that MRX-I is first oxidized to an enol lactone via the Baeyer–Villiger ring-expanding reaction, specifically catalyzed by FMO5, followed by its hydrolysis to an enol, and then transformation to an aldehyde intermediate by enol–aldehyde tautomerism. The aldehyde is reduced by SDR, AKR and ALDH to MRX445-1 or oxidized to MRX459 by ALDH. Our study demonstrated that the main metabolic pathway of MRX-I, via the opening of the DHPO ring, is not catalyzed by P450s, the enzymes primarily responsible for metabolizing drugs and xenobiotics, but by multiple other enzymes, including FMO5, SDR, AKR, ALDH and AO. Therefore, few clinical adverse drug–drug interactions should be anticipated between MRX-I and P450 inhibitors or inducers.

Acknowledgments

We would like to thank the staff of Clinical Trial Center of Shanghai Huashan Hospital and the volunteers in the clinical study

Authorship Contributions

Participated in research design: Jian Meng, Dafang Zhong, Zhengyu Yuan, Xiaoyan Chen

Conducted experiments: Jian Meng, Liang Li, Hong Yuan, Jialan Zhou, Chen Li

Performed data analysis: Jian Meng, Liang Li, Cen Xie, Mikhail Fedorovich Gordeev, Jinqian Liu,

Xiaoyan Chen

Wrote or contributed to the writing of the manuscript: Jian Meng, Liang Li, Xiaoyan Chen

References

- Benedetti MS, Whomsley R, and Baltes E (2006) Involvement of enzymes other than CYPs in the oxidative metabolism of xenobiotics. *Expert Opin Drug Metab Toxicol* **2**:895–921.
- Brickner SJ, Barbachyn MR, Hutchinson DK, and Manninen PR (2008) Linezolid (ZYVOX), the first member of a completely new class of antibacterial agents for treatment of serious Gram-positive infections. *J Med Chem* **51**:1981–1990.
- Cashman JR (2008) Role of flavin-containing monooxygenase in drug development. *Expert Opin Drug Metab Toxicol* **4**:1507–1521.
- Dean S (1999) Mechanism of action of the oxazolidinone antibacterial agents. *Expert Opin Investig Drugs* **8**:1195–1202.
- Gordeev MF, and Yuan ZY (2014) New potent antibacterial oxazolidinone (MRX-I) with an improved class safety profile. *J Med Chem* **57**:4487–4497.
- Krafft GA and Katzenellenbogen JA (1981) Synthesis of haloenol lactones, mechanism-based inactivators of serine proteases. *J Am Chem Soc* **103**:5459–5466.
- Lai WG, Farah N, Moniz GA, and Wong YN (2011) A Baeyer-Villiger oxidation specifically catalyzed by human flavin-containing monooxygenase 5. *Drug Metab Dispos* **39**:61–70.
- Li CR, Zhai QQ, Wang XK, Hu XX, Li GQ, Zhang WX, Pang J, Lu X, Yuan H, Gordeev MF, Chen LT, Yang XY, You XF (2014) *In vivo* antibacterial activity of MRX-I, a new oxazolidinone. *Antimicrob Agents Chemother* **58**:2418–2421.

- Morrison RD, Blobaum AL, Byers FW, Santomango TS, Bridges TM, Stec D, Brewer KA, Sanchez-Ponce R, Corlew MM, Rush R, Felts AS, Manka J, Bates BS, Venable DF, Rodriguez AL, Jones CK, Niswender CM, Conn PJ, Lindsley CW, Emmitte KA, and Daniels JS (2010) The role of aldehyde oxidase and xanthine oxidase in the biotransformation of a novel negative allosteric modulator of metabotropic glutamate receptor subtype 5. *Drug Metabo Dispos* **38**:667–678.
- Nagiec EE, Wu L, Swaney SM, Chosay JG, Ross DE, Brieland JK, and Leach KL (2005) Oxazolidinones inhibit cellular proliferation via inhibition of mitochondrial protein synthesis. *Antimicrob Agents Chemother* **49**:3896–3902.
- Overby LH, Carver GC, and Philpot RM (1997) Quantitation and kinetic properties of hepatic microsomal and recombinant flavin-containing monooxygenases 3 and 5 from humans. *Chem Biol Interact* **106**:29–45.
- Rosemond MJC, and Walsh JS (2004) Human carbonyl reduction pathways and a strategy for their study *in vitro*. *Drug Metab Rev* **36**:335–361.
- Shono T, Matsumura Y, Hibino K, and Miyawaki S (1974) A novel synthesis of 1-citronellol from 1-menthone. *Tetrahedron Let* **1295**:1295–1298.
- Stagos D, Chen Y, Brocker C, Donald E, Jackson BC, Orlicky DJ, Thompson DC, and Vasiliou V (2010) Aldehyde dehydrogenase 1B1: molecular cloning and characterization of a novel mitochondrial acetaldehyde-metabolizing enzyme. *Drug Metabo Dispos* **38**:1679–1687.
- Talbot GH, Bradley J, Edwards JE, Gilbert D, Scheld M, and Bartlett JG (2006) Bad bugs need drugs: an update on the development pipeline from the antimicrobial

availability task force of the infectious diseases society of america. *Clin Infect Dis* **42**:657–668.

Uetrecht JP and Targher W (2007) *Drug Metabolism: Chemical and Enzymetic Aspects*, pp 61, Informa Healthcare, New York

Vinh DC, and Rubinstein E (2009) Linezolid: a review of safety and tolerability. *J Infect* **59**:S59–S74.

Vos RME (1998) *In vitro* and *in vivo* metabolism of the progestagen ORG 30659 in several species. *Drug Metab Dispos* **26**:1102–1112.

Zhang J, and Cashman JR (2006) Quantitative analysis of FMO gene mRNA levels in human tissues. *Drug Metab Dispos* **34**:19–26

Scheme Legends

Scheme 1. Proposed metabolic pathway of MRX-I in humans.

Scheme 2. Proposed metabolic pathway for the formation of MRX445 from MRX-I by analogy with previous studies (Lai et al., 2011; Verhoeven et al., 1998).

Scheme 3. Proposed mechanism for the formation of MRX445-1, MRX445-2, and MRX459 from MRX-I in the presence of H₂¹⁸O.

Scheme 4. Proposed mechanism for the formation of MRX445-1 and MRX-1315 from MRX-1314 in the presence of H₂¹⁸O.

Figure Legends

Fig. 1. Metabolite profile of human plasma 1.5 hours after the oral administration of 600 mg MRX-I, detected by UPLC/Triple TOF MS (A) and UPLC-UV chromatograms of pooled plasma (B) and blank plasma (C). AU, arbitrary units. The inset is the expanded chromatogram in the region of 13–18 minutes.

Fig. 2. Metabolite profile of human urine 0–24 hours after the oral administration of 600 mg MRX-I, detected by UPLC/Triple TOF MS (A) and UPLC-UV chromatograms of pooled urine (B) and blank urine (C). AU, arbitrary units.

Fig. 3. Metabolite profile of human feces 0–24 hours after the oral administration of 600 mg MRX-I, detected by UPLC/Triple TOF MS (A) and UPLC-UV chromatograms of pooled feces (B) and blank feces (C). AU, arbitrary units.

Fig. 4. Metabolite profiles of MRX-I incubated with human liver microsomes (A), cytosol (B), and S9 fractions (C) for 120 minutes detected by UPLC/ Triple TOF MS.

Fig. 5. UPLC/Triple TOF MS extracted ion chromatograms (EIC) of MRX445-1,

MRX445-2, and MRX459 in samples after MRX-I was incubated for 120 minutes with human liver cytosol-fortified FMO1 (A), FMO3 (B), and FMO5 (C). Data were filtered to show only MRX445-1, MRX445-2 (m/z 445.133 \pm 0.010 Da), and MRX459 (m/z 459.123 \pm 0.010 Da).

Fig. 6. MS/MS spectra of MRX445-1 (A, formed from MRX-I in H₂¹⁶O; B, formed from MRX-I in H₂¹⁸O; C, formed from MRX-1314 in H₂¹⁸O), MRX445-2 (D, formed from MRX-I in H₂¹⁶O; E, formed from MRX-I in H₂¹⁸O), and MRX459 (F, formed from MRX-I in H₂¹⁶O; G, formed from MRX-I in H₂¹⁸O) in samples of MRX-I or MRX-1314 was incubated for 120 minutes with liver cytosol-fortified FMO5.

Fig. 7. Metabolite profiles of MRX-I (A) or MRX-1314 (B) incubated with human hepatocytes for 120 minutes detected, by UPLC/Q-TOF MS.

TABLE 1 Mass spectral fragmentation and structures of MRX-I and its proposed metabolites (Mass spectra of MRX-I and metabolites shown in Supplemental Figure S1).

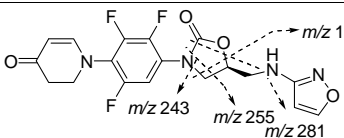
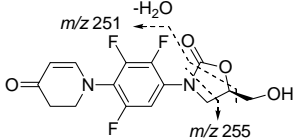
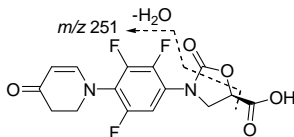
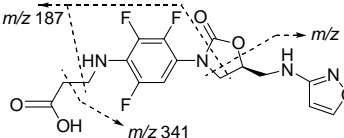
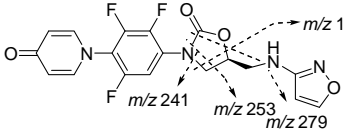
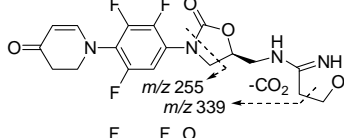
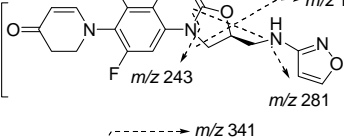
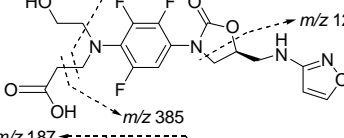
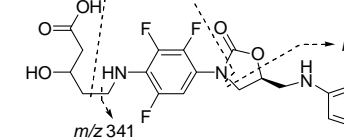
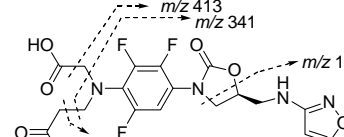
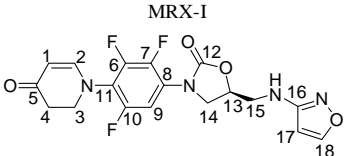
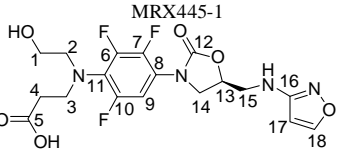
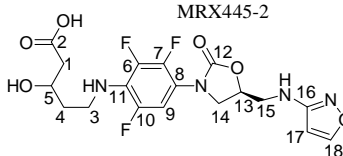
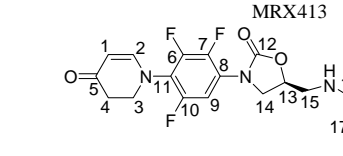
	Structure	t_R (min)	$[M + H]^+$	Characteristic Fragment Ions
M0 (MRX-I)		17.2	409.1111	365.1219 ($-CO_2$), 281.0899, 255.0749, 243.0736, 123.0549
MRX343		14.1	343.0895	325.0795 ($-H_2O$), 255.0737, 251.0788
MRX357		15.1	357.0693	339.0587 ($-H_2O$), 251.0787
MRX401		17.1	401.1070	341.0860, 187.0471, 123.0547
MRX407		14.2	407.0962	363.1061 ($-CO_2$), 279.0737, 253.0585, 241.0579, 123.0553
MRX413		9.30	413.1428,	369.1528 ($-CO_2$), 339.1426, 255.0733
MRX427		13.6	427.1227	409.1119 ($-H_2O$), 368.0851 ($-C_2H_5NO$), 281.0889, 243.0727, 123.0538
MRX445-1		16.2	445.1322	427.1224 ($-H_2O$), 385.1109, 341.0863, 123.0555
MRX445-2		16.7	445.1316	427.1212 ($-H_2O$), 409.1095 ($-2H_2O$), 341.0855, 187.0465, 123.0544
MRX459		16.1	459.1114	413.1059, 399.0902, 341.0848, 187.0473, 123.0551

TABLE 2 ¹H NMR chemical shift assignments for MRX-I, MRX445-1, MRX445-2, and MRX413 (NMR spectra shown in Supplemental Figure S2 – S5).

Chemical Shift (ppm) for				
	MRX-I	MRX445-1	MRX445-2	MRX413
Protons				
1	5.07, d (<i>J</i> = 7.8 Hz)	3.14, t (<i>J</i> = 5.7 Hz, 2H)	2.34, dd <i>J</i> = 15.2, 5.4 Hz; 2.27, dd, <i>J</i> = 15.2, 7.8 Hz	5.26, d, <i>J</i> = 7.7 Hz
2	7.48, d (<i>J</i> = 7.8 Hz)	3.20-3.50, m (6H)		7.44, d, <i>J</i> = 7.7 Hz
3	3.88, m	3.20-3.50, m (6H)	3.70, m	3.97, t, <i>J</i> = 7.5 Hz
4	2.51, t (<i>J</i> = 7.4 Hz, 2H)	2.33, t (<i>J</i> = 6.4 Hz, 2H)	1.67, m; 1.55, m	2.45, t, <i>J</i> = 7.6 Hz, 2H
5			3.92, m	
9	7.56, m	7.26, m	7.18, m	7.51, m
13	4.95, m	4.88, brs	4.88, m	5.02, m
14	3.88, m; 4.18, t (<i>J</i> = 8.6 Hz)	4.08, t (<i>J</i> = 8.5 Hz); 3.77, dd (<i>J</i> = 7.8, 6.7 Hz)	3.92, m; 4.02, t (<i>J</i> = 8.6 Hz)	4.27, t, <i>J</i> = 8.9 Hz; 3.93, t, <i>J</i> = 6.9 Hz
15	3.48, t (<i>J</i> = 5.4 Hz, 2H)	3.20-3.50, m (6H)	3.44, m	3.81, dd, <i>J</i> = 14.9, 3.4 Hz; 3.72, dd, <i>J</i> = 14.9, 6.9 Hz
17	6.02, d (<i>J</i> = 1.8 Hz)	5.99, m	6.02, d (<i>J</i> = 1.2 Hz)	2.72, t, <i>J</i> = 5.9 Hz
18	8.41, d (<i>J</i> = 1.8 Hz)	8.37, brs	8.41, d (<i>J</i> = 1.2 Hz)	3.88, dd, <i>J</i> = 5.8, 1.5 Hz, 2H
NH	6.59, t (<i>J</i> = 6.0 Hz)	6.54, brt (<i>J</i> = 5.5 Hz)	6.59, t (<i>J</i> = 5.9 Hz); 5.61, brs	

d, doublet; q, quartet; m, multiplet; s, singlet; t, triplet

TABLE 3 ^{13}C NMR chemical shift assignments for MRX-I, MRX445-1, MRX445-2, and MRX413 (NMR spectra shown in Supplemental Figure S2 – S5).

Carbon	Chemical Shift (ppm)			
	MRX-I	MRX445-1	MRX445-2	MRX413
1	102.5, d	59.8, t	37.8, t	101.4, d
2	152.5, d	55.4, t	173.5, s	153.5, d
3	49.6, t	49.3, t	43.1, t	49.2, t
4	36.5, t	33.6, t	42.3, t	35.4, t
5	191.1, s	173.4, s	65.7, d	193.6, s
6	145.5-148.0, d	147.1-149.1, d	146.2-148.0, d	
7	141.2-143.6, d	141.9-143.9, d	139.8-141.7, d	
8	125.5, s	126.8, s	127.2, s	125.1, s
9	108.5, d	108.6, d	109.5, d	108.1, d
10	151.3-153.7, d	153.3-155.2, d	153.3-155.1, d	
11	121.8, s	121.9, s	113.5, s	121.5, s
12	154.9, s	155.2, s	155.7, s	154.9, s
13	73.3, d	73.0, d	72.8, d	72.2, d
14	49.3, t	49.1, t	49.7, t	48.6, t
15	46.4, t	46.3, t	46.5, t	48.5, t
16	164.3, s	164.2, s	164.2, s	168.1, s
17	96.9, d	96.9, d	97.0, d	35.9, t
18	159.0, d	159.0, d	159.1, d	58.2, t

d, CH or CF; q, CH₃; s, C; t, CH₂

TABLE 4 Effects of enzyme inhibition on the formation of MRX445-1, MRX445-2, and MRX459 from MRX-I (10 μ M) in human liver S9 fractions (protein concentration, 2.5 mg/ml).

Inhibitor or Process	Inhibitor Concentration (μ M)	Target Enzyme	Metabolite Formation (%)		
			MRX445-1	MRX445-2	MRX459
No inhibitor (Control)			100	100	100
ABT ^a	1000	P450s	91.2	91.6	88.7
Methimazole ^a	100	P450s, FMO1, FMO2, FMO3 and FMO4	92.0	94.8	97.8
Heated ^a	–	FMO1, FMO3, FMO4, FMO5	7.22	90.0	n. d.
Menadione ^a	10	AO and SDR	44.6	42.9	107
Raloxifene ^a	10	AO	83.1	19.9	98.0
Methotrexate ^a	50	XO	90.2	88.3	106
Allopurinol ^a	100	XO	110	103	94.2
Flufenamic acid ^a	100	AKR	69.4	75.2	88.1
4-MP ^b	100	ADH	103	88.5	93.3
Disulfiram ^c	50	ALDH	80.0	57.1	10.7

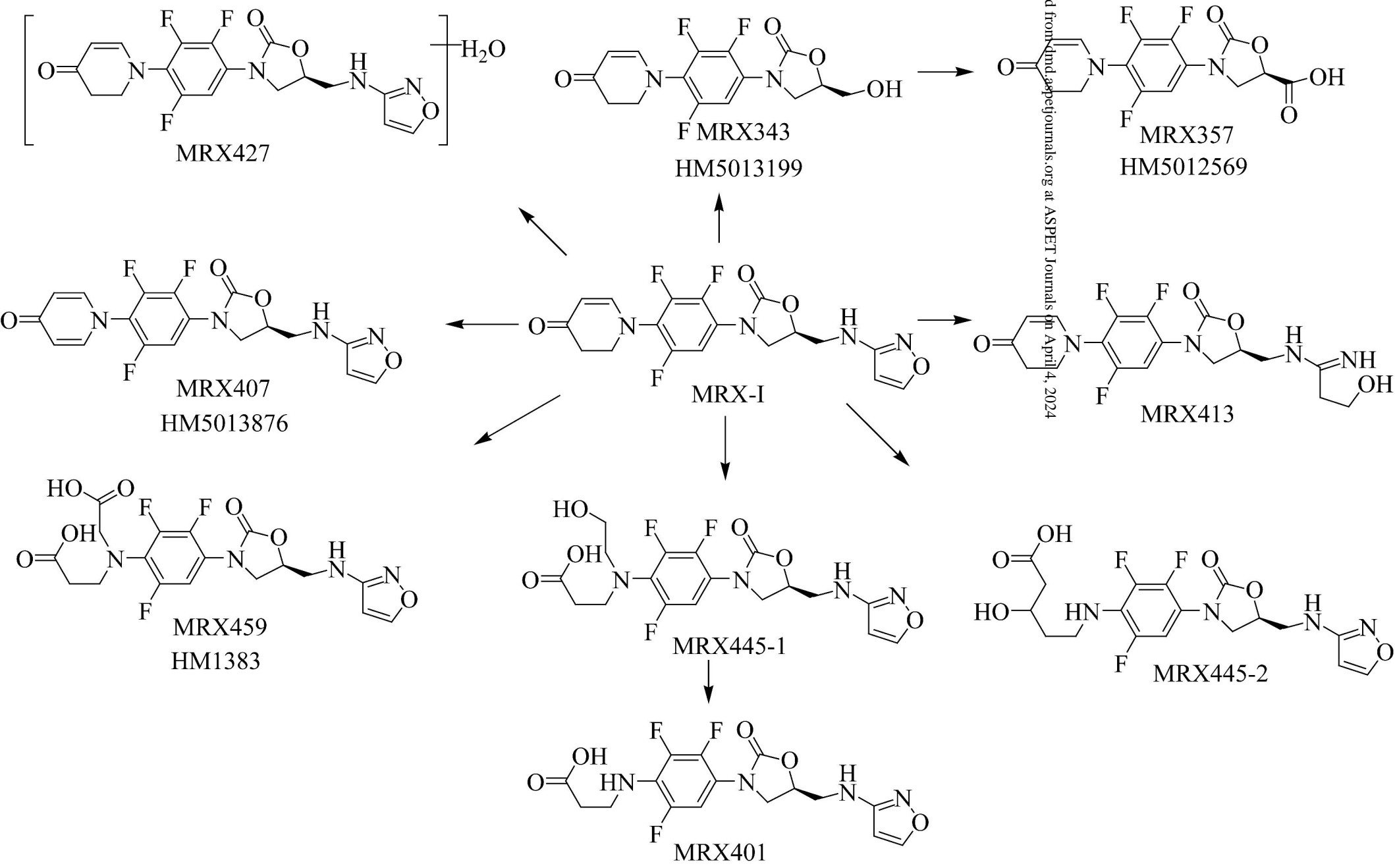
n.d., Not detected.

^aNADPH (2.0 mM) was supplemented as coenzyme.

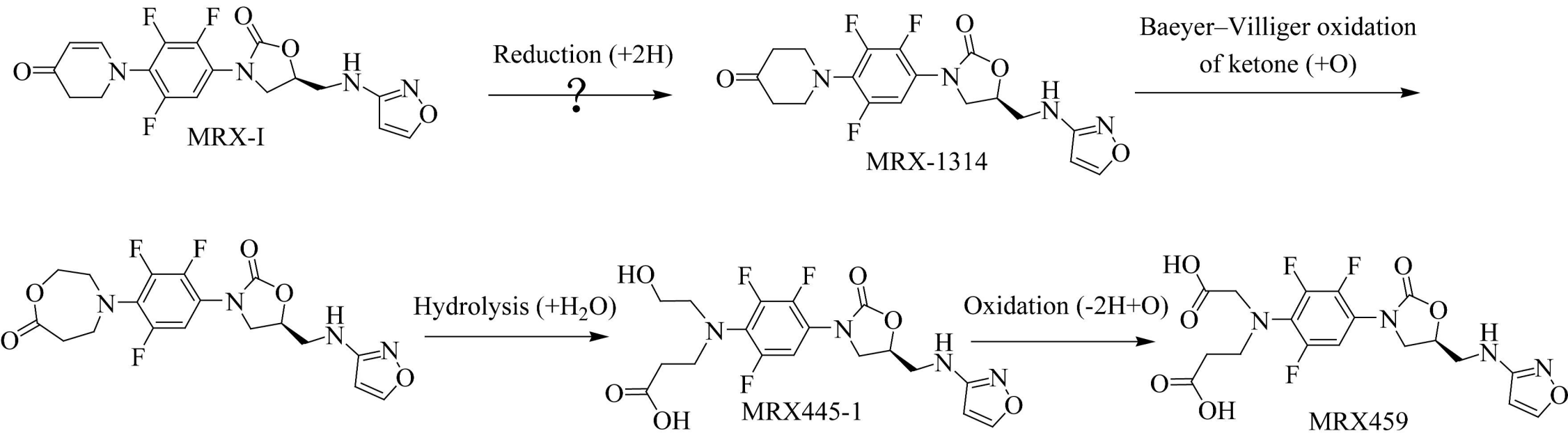
^bNADPH (2.0 mM) and NAD⁺ (2.0 mM) were supplemented as coenzyme.

^cNADPH (2.0 mM) and NADP⁺ (2.0 mM) were supplemented as coenzyme.

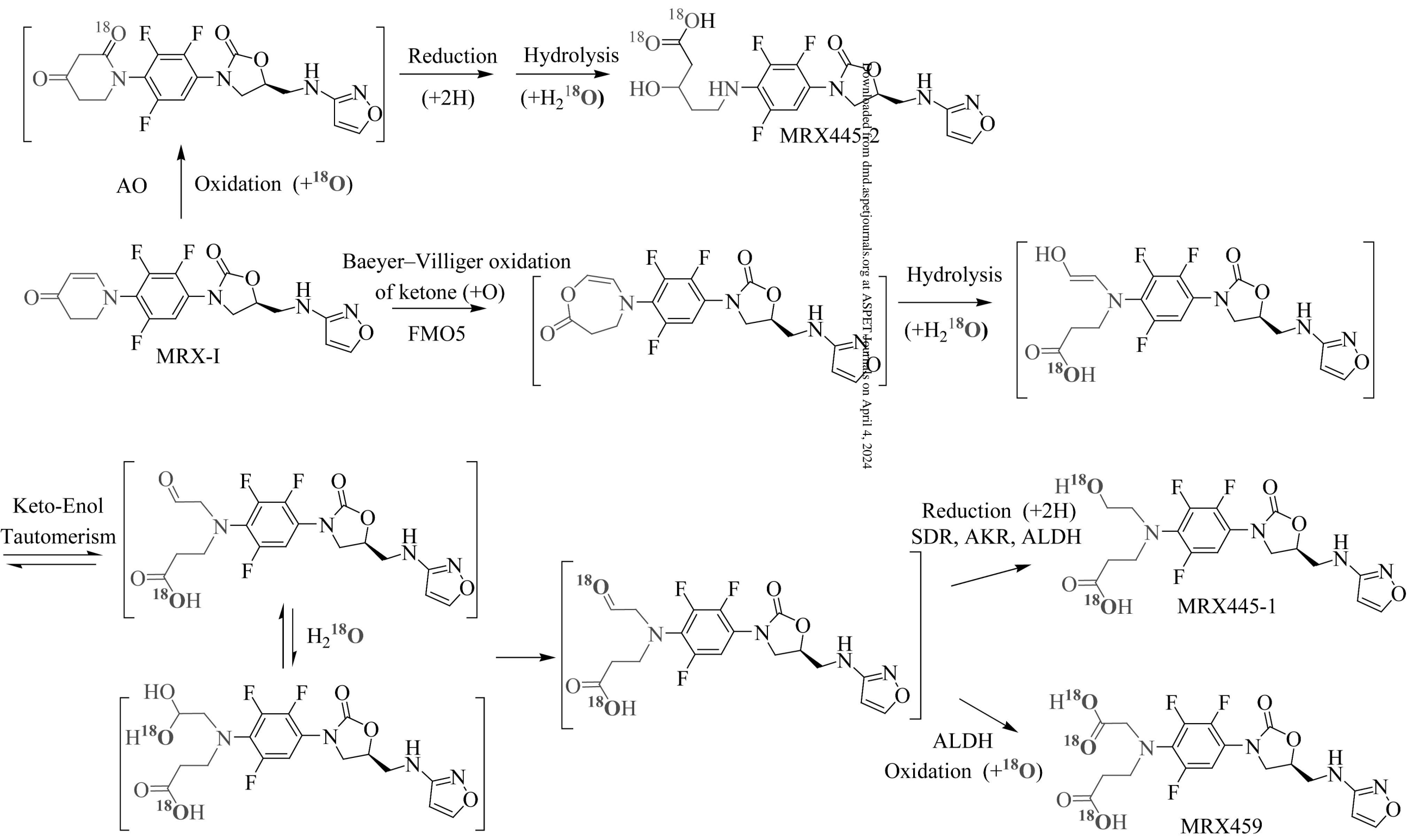
Scheme 1



Scheme 2



Scheme 3



Scheme 4

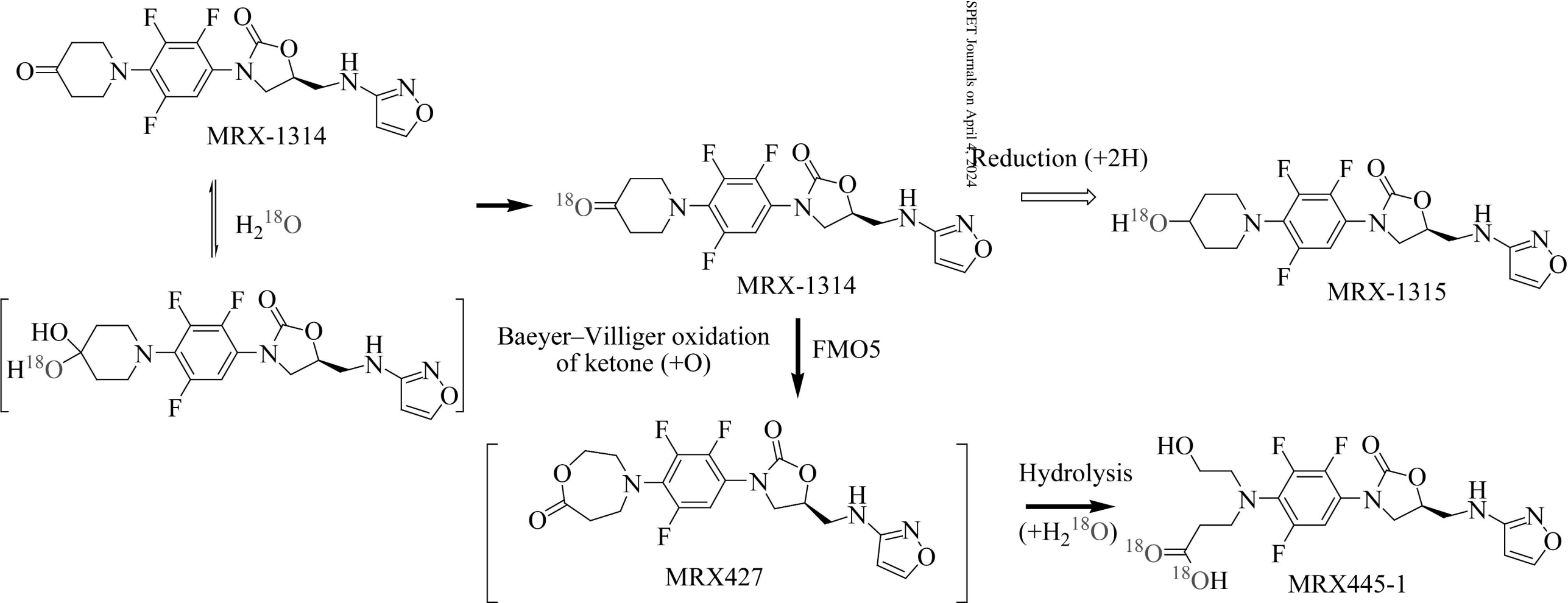


Figure 1

Metabolite Chromatogram

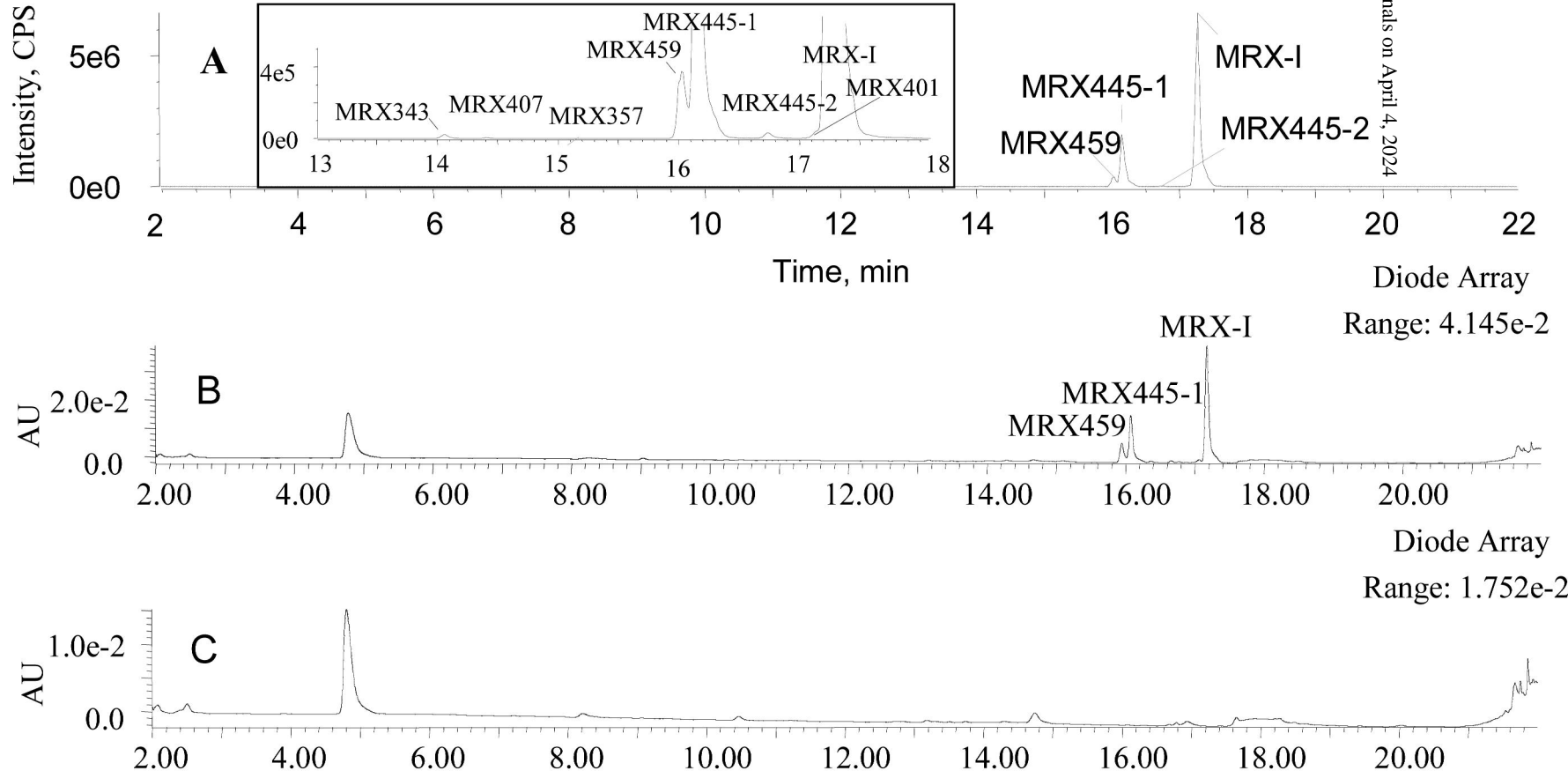


Figure 2
Metabolite Chromatogram

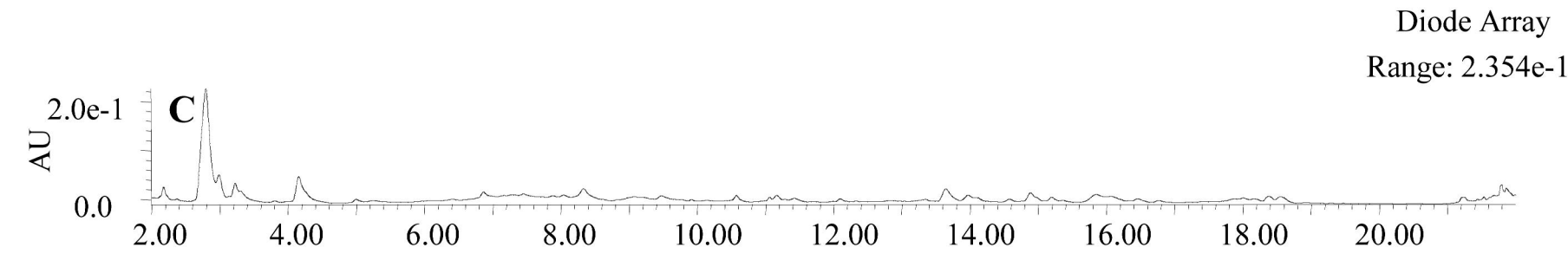
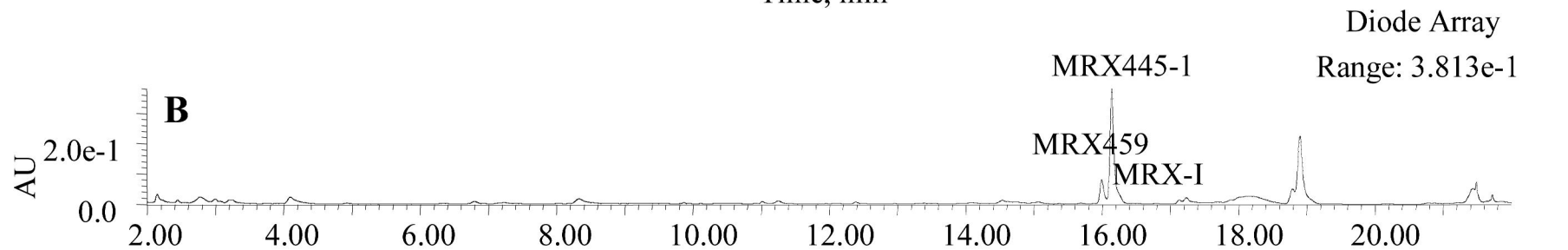
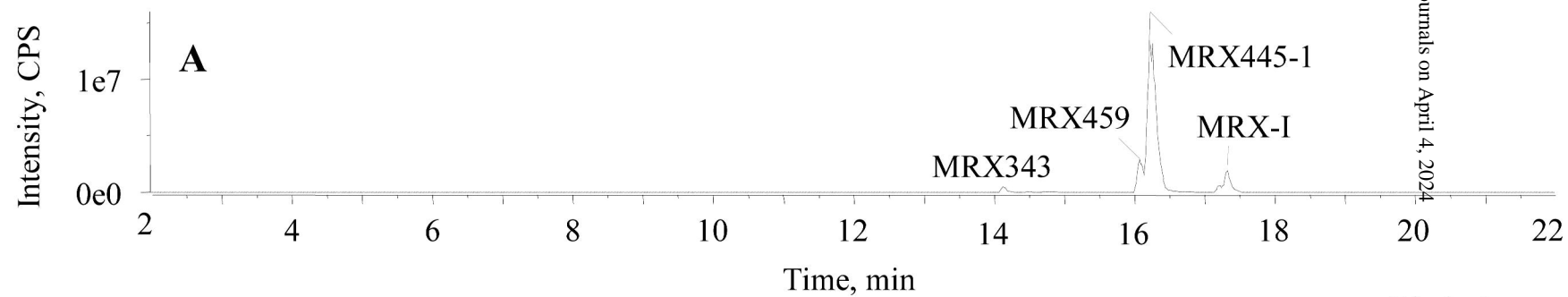


Figure 3
Metabolite Chromatogram

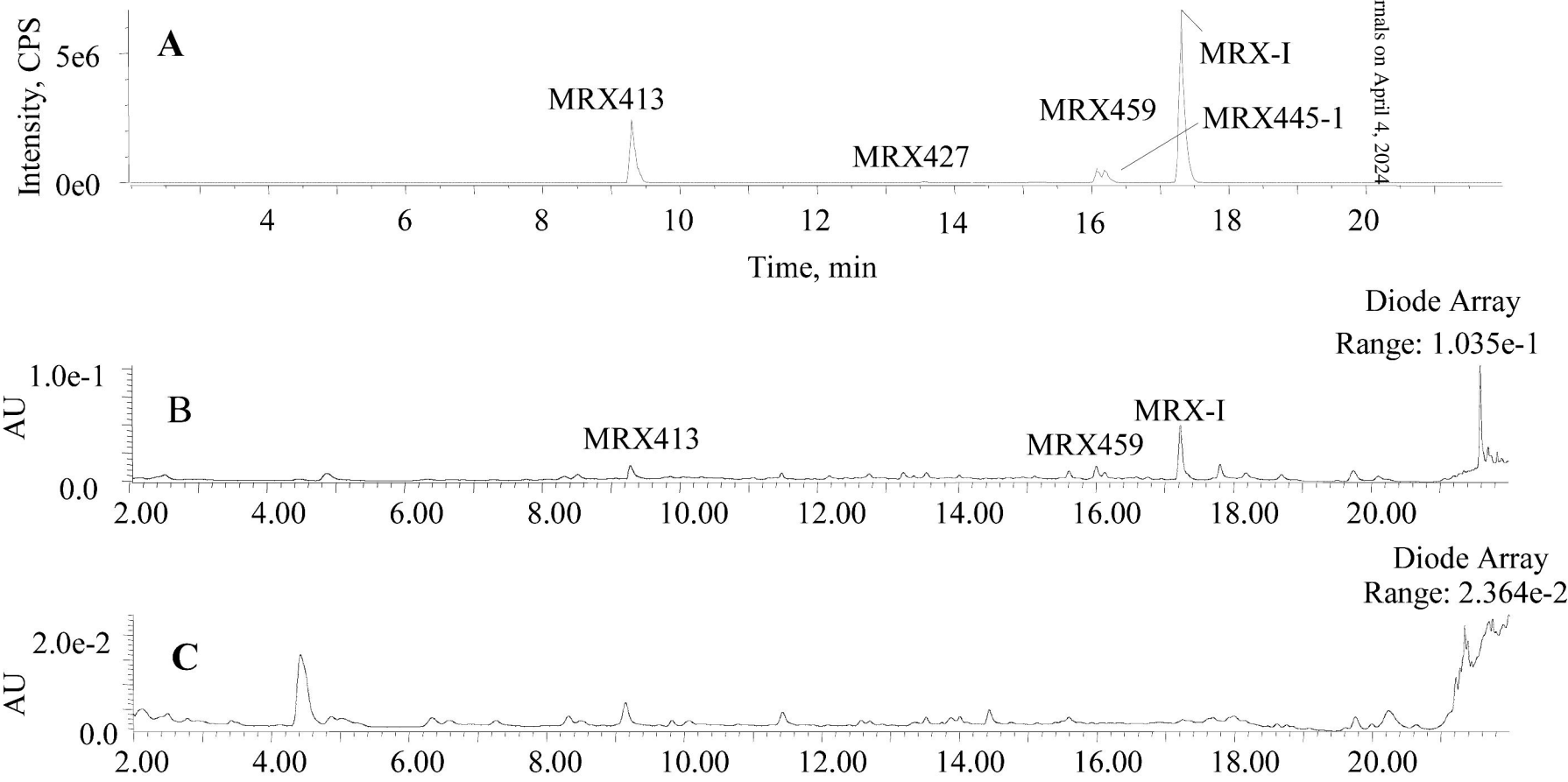
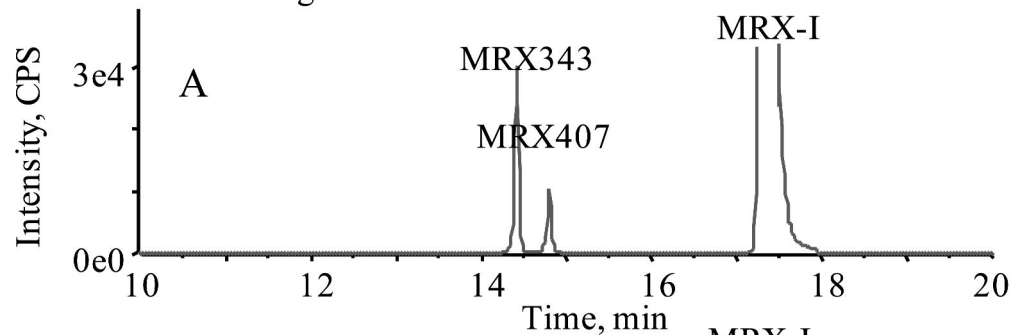
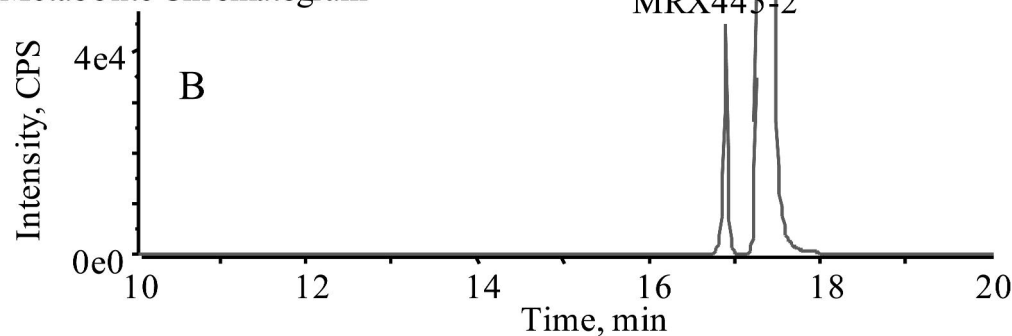


Figure 4

Metabolite Chromatogram



Metabolite Chromatogram



Metabolite Chromatogram

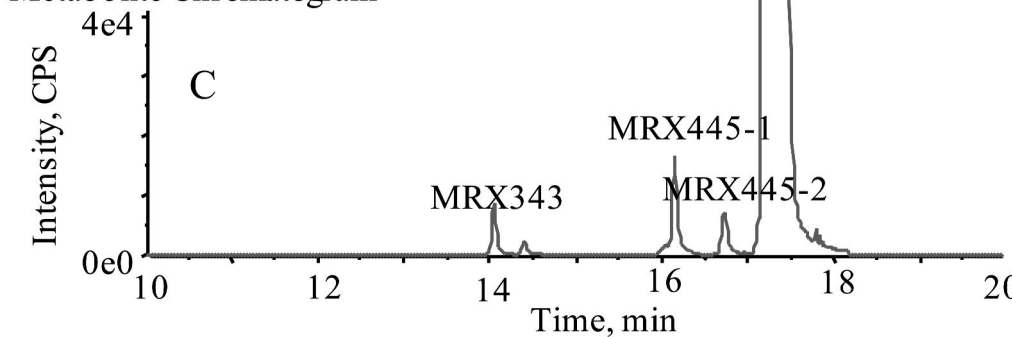


Figure 5

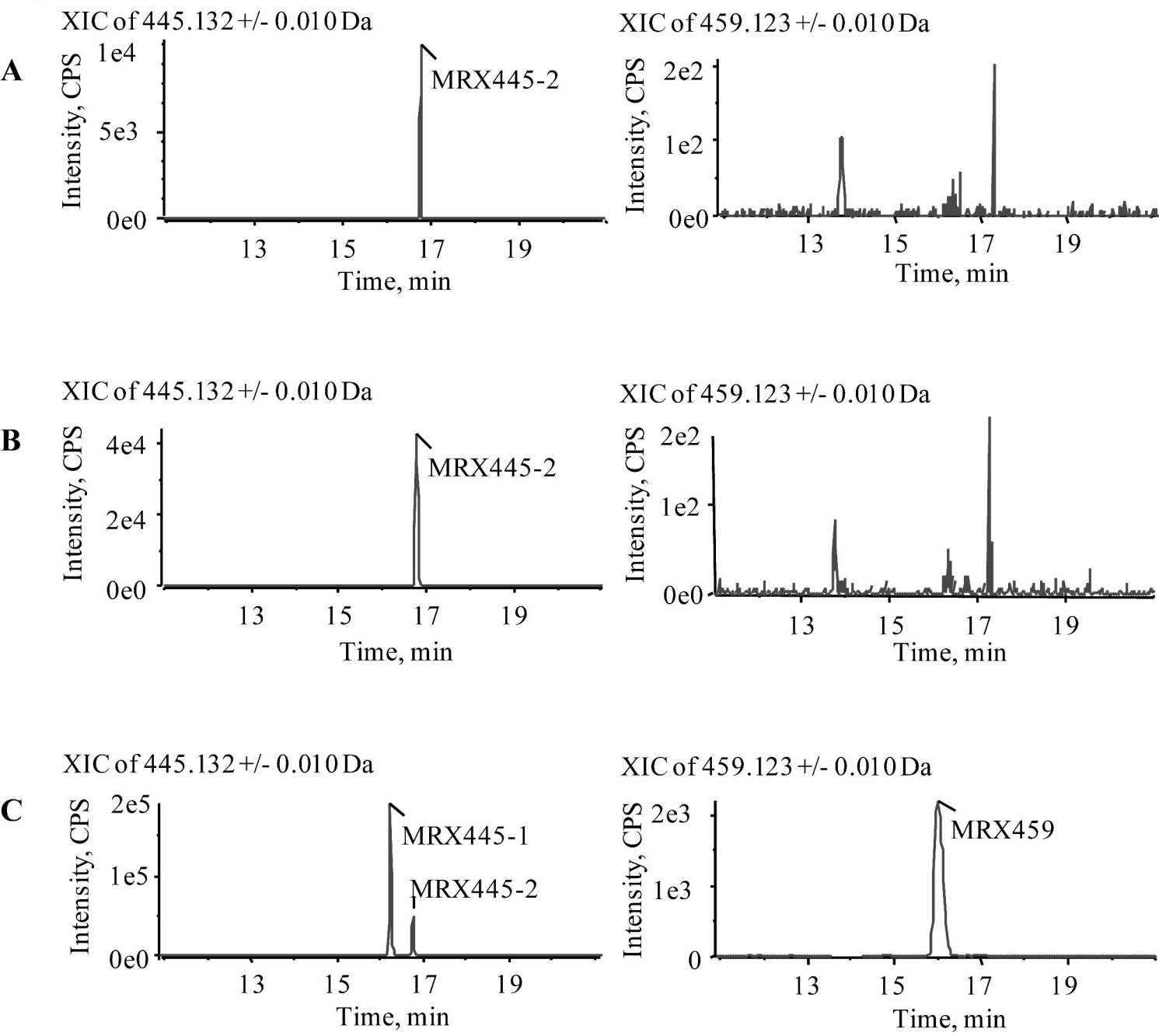
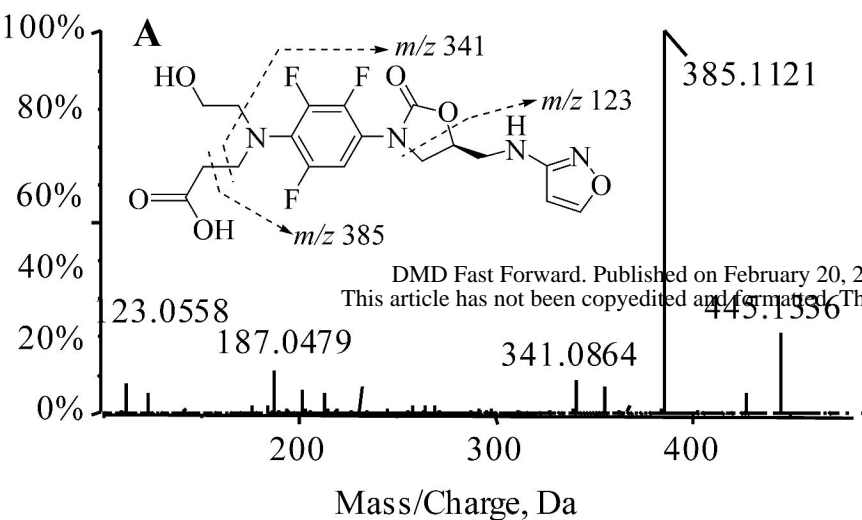
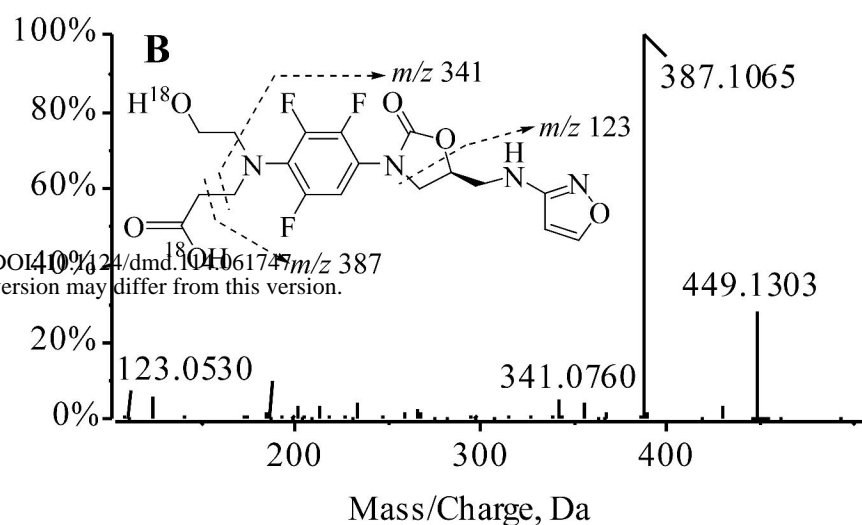


Figure 6

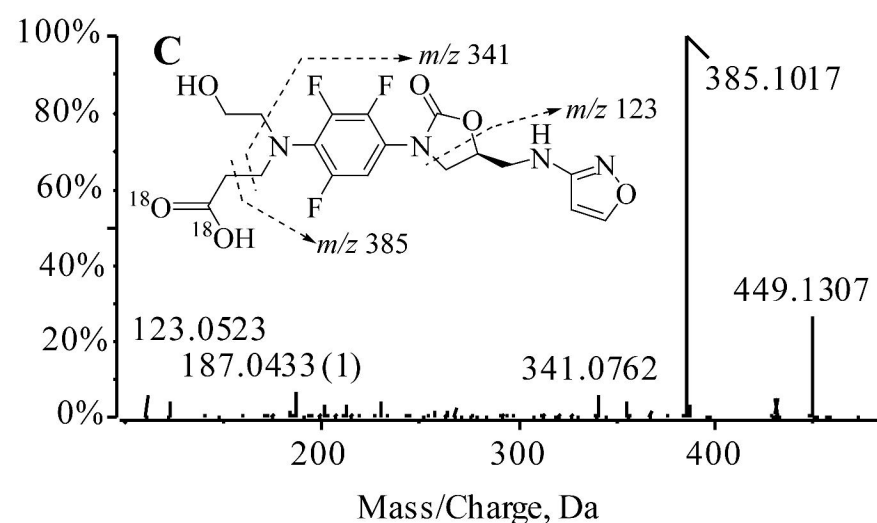
Precursor: 445.1 Da, CE: 35.0



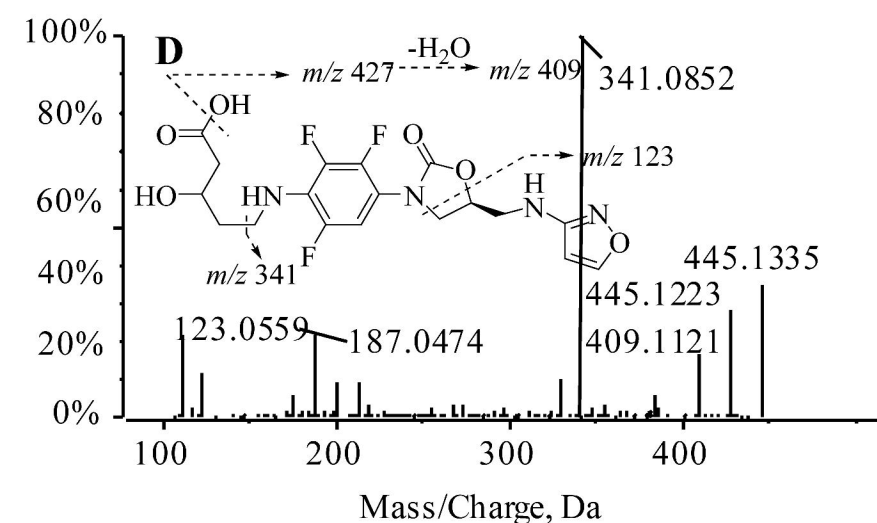
Precursor: 449.1 Da, CE: 35.0



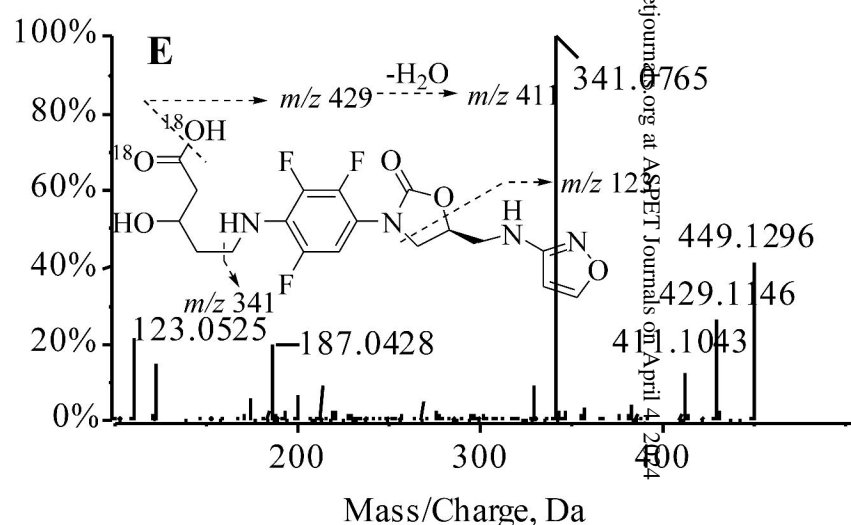
Precursor: 449.1 Da, CE: 35.0



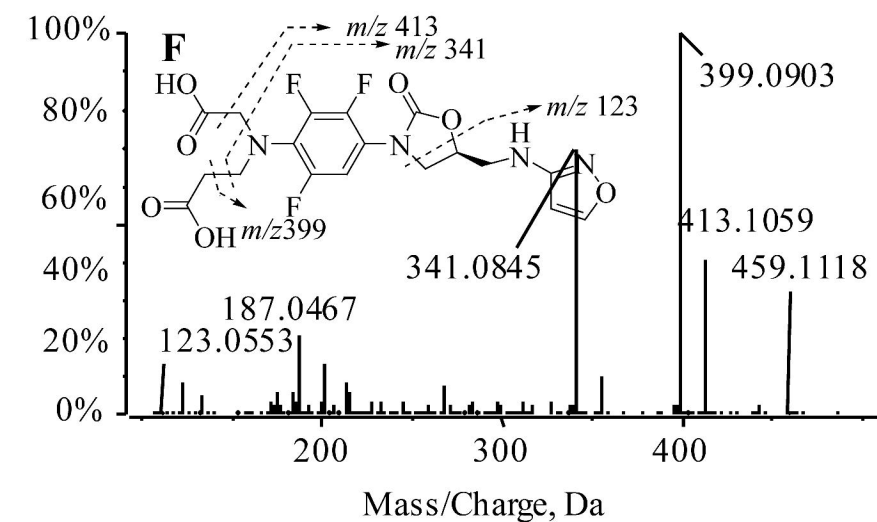
Precursor: 445.1 Da, CE: 35.0



Precursor: 449.1 Da, CE: 35.0



Precursor: 459.1 Da, CE: 35.0



Precursor: 465.1 Da, CE: 35.0

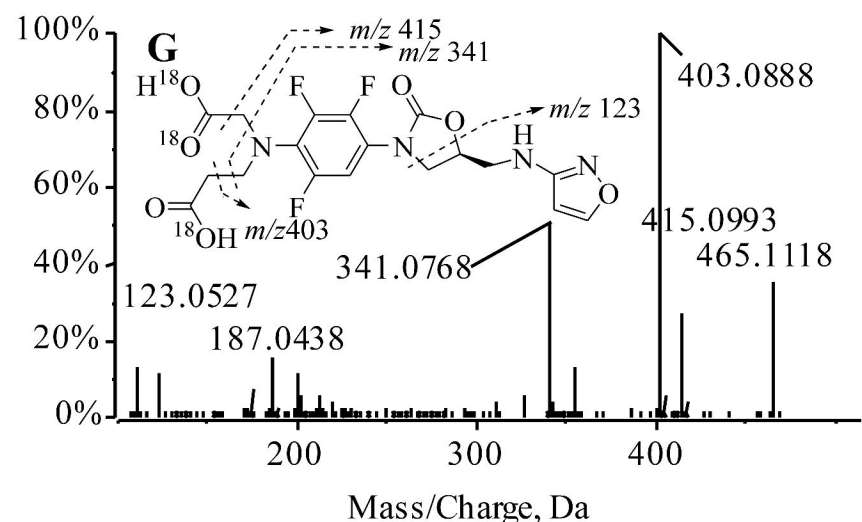
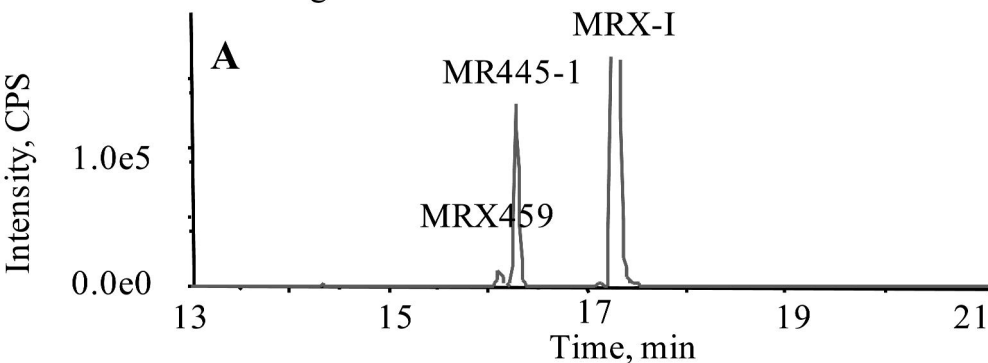


Figure 7

Metabolite Chromatogram



Metabolite Chromatogram

